



MAPP Phase-1 Technical Proposal

Version 2.1

November 23rd 2021

B. Acharya,^{1,2} J. Alexandre,¹ P. Benes,³ B. Bergmann,³ J. Bertolucci,⁸ A. Bevan,⁵ R. Bhattacharya,⁸ H. Branzas,⁶ P. Burian,³ M. Campbell,⁷ M. Campbell,⁷ S. Cecchini,⁸ Y. M. Cho,²⁵ M. de Montigny,⁹ A. de Roeck,⁷ J. R. Ellis,^{1,10} M. Fairbairn,¹ D. Felea,⁶ M. Frank,¹⁰ J. Hays,⁵ A. M. Hirt,²⁶ P.Q. Hung,²⁷ J. Janecek,³ M. Kalliokoski,¹⁷ D-W D. Lacarère,⁷ C. Leroy,¹⁵ G. Levi,⁸ A. Lioni,¹⁴ A. S. Lobos,⁹ A. Margiotta,¹⁷ R. Maselek,¹² A. Maulik,^{8,9} N. Mauri,⁸ N. E. Mavromatos,¹ M. Mieskolainen,¹⁷ L. Millward,⁵ V. A. Mitsou,⁴ R. Oravo,¹⁷ I. Ostrovskiy,¹⁸ P.-P. Ouimet,⁹ J. Papavassilou,⁴ B. Parker,¹⁹ L. Patrizii,⁸ G. E. Pávālas,⁶ J. L. Pinfold,^{9,*} L. A. Popa,⁶ V. Popa,⁶ M. Pozzato,⁸ S. Pospisil,³ A. Rajantie,²¹ R. Ruiz de Austi,⁴ Z. Sahnoun,^{8,21} M. Sakellariadou,¹ K. Sakurai,¹² A. Santra,⁴ S. Sarkar,¹ G. Semenov,²² A. Shaa,²³ G. Sirri,⁸ K. Sliwa,²³ R. Soluk,⁹ M. Spurio,⁸ M. Staelens,⁹ M. Suk,⁴ M. Tenti,²⁴ V. Togo,⁸ J. A. Tuszyński,⁹ A. Upreti,¹⁸ V. Vento,⁴ O. Vives,⁴

¹Theoretical Particle Physics & Cosmology Group, Physics Dept., King's College London, UK

²International Centre for Theoretical Physics, Trieste, Italy

³IEAP, Czech Technical University in Prague, Czech Republic

⁴IFIC, Universitat de València - CSIC, València, Spain

⁵School of Physics and Astronomy, Queen Mary University of London, London, England

⁶Institute of Space Science, Bucharest - Măgurele, Romania

⁷Experimental Physics Department, CERN, Geneva, Switzerland

⁸INFN, Section of Bologna, Bologna, Italy

⁹Physics Department, University of Alberta, Edmonton, Alberta, Canada

¹⁰Department of Physics, Concordia University, Montréal, Quebec, Canada

¹¹Physics Department, University of Muenster, Muenster, Germany

¹²Institute of Theoretical Physics, University of Warsaw, Warsaw, Poland

¹³Physics Department, University of Cincinnati, Cincinnati, Ohio, USA

¹⁴Section de Physique, Université de Genève, Geneva, Switzerland

¹⁵Physics Department, Université of Montréal, Montréal, Quebec, Canada

¹⁶INFN, Section of Bologna & Department of Physics & Astronomy, University of Bologna, Italy

¹⁷Physics Department, University of Helsinki, Helsinki, Finland

¹⁸Physics Department, University of Alabama, Tuscaloosa, Alabama, USA

¹⁹The Institute for Research in Schools, Canterbury, England

²⁰Department of Physics, Imperial College London, UK

²¹Centre for Astronomy, Astrophysics and Geophysics, Algiers, Algeria

²²Department of Physics, University of British Columbia, Vancouver, British Columbia, Canada

²³Department of Physics and Astronomy, Tufts University, Medford, Massachusetts, USA

²⁴INFN, CNAF, Bologna, Italy

²⁵Centre for Quantum Spacetime, Sogang University, Seoul, Korea

²⁶Department of Earth Sciences, Swiss Federal Institute of Technology, Zurich, Switzerland

²⁷Department of Physics, University of Virginia, Charlottesville, Virginia, USA

* Communicating Author E-mail: jpinfold@ualberta.ca



Abstract

This is the Technical Proposal for Phase-1 of the MoEDAL Apparatus for Penetrating Particles (MAPP-1) to be installed in UA83 at IP8, The main purpose of this upgrade is to expand the physics reach of the MoEDAL detector to include sensitivity to Feebly (electromagnetically) Interacting Particles (FIPs), such as milli-charged messengers of new physics. However, the MAPP-mCP detector will also have some sensitivity to weakly interacting neutral long-lived particles. Additionally, The MAPP-1 detector will be utilized to monitor MoEDAL trapping volumes for the presence of extremely Long-Lived Charged Particles (LLCPs). Phase-2 of the program, that will be the subject of a future Technical Proposal, would see the deployment of the MAPP-2 detector in the UGC1 gallery to greatly expand the sensitivity to the decays of very long-lived neutral particles at the High Luminosity LHC.

Contents

1	Introduction	3
2	The Phase-1 MAPP-mCP Upgrade	6
2.1	The MAPP - mCP Detector	6
2.1.1	MAPP- mCP Mechanics	6
2.1.2	The MAPP-mQP Calibration System	6
2.1.3	The MAPP-mQP Veto System	9
2.1.4	MAPP-mQP Radiator Layers	10
2.1.5	MAPP-mQP Frontend, HV, DAQ and Trigger	10
3	The MAPP-mCP Deployment in the UA83 Tunnel	13
3.1	Staging and Temporary Storage Area	13
3.2	Beam Induced Radiation Backgrounds in the MAPP-mCP Region of the UA83 Tunnel	13
3.3	Beam Induced Backgrounds in the MAPP-mCP detector in UA83	14
3.4	Installation of Required Infrastructure	15
4	Safety Matters	18
4.1	UA83 Tunnel Safety Issues	18
4.2	Safety Issues Relating to the MAPP-mCP Detector	18
4.2.1	Readout Electronics and HV	18
4.2.2	The Scintillator Detectors and Their Support Structure	18
4.2.2.1	The Flame Shield	19
4.2.3	Presence of Lead in the Radiator Layers	19
4.3	Safety Issues Relating to Detector Installation	19
4.4	Safety Monitoring After Detector Installation	20
4.5	MoEDAL-MAPP Safety Organization	20
5	Construction and Installation of the Phase-1 MAPP Detector	21
5.1	Organization of Construction, Installation and Running of the Detector	21
5.2	Construction of the Detector	22
5.3	MAPP-mCP Detector Installation	22
6	Maintenance and Operation of the MAPP Detector During Run-3	24
6.1	The MAPP Control Centre	24
7	Funding Plans for the MoEDAL-MAPP Phase-1 Installation	25
8	Physics Issues	25
8.1	The Full Simulation of the UA83, MoEDAL, MAPP-mCP Arena (SUMMA)	25
8.2	Some Physics Benchmarks	26
8.2.1	Mini-Charged Particles from Dark QED	26
8.2.1.1	Backgrounds	27
8.2.2	Detecting the EDM of Exotic Particles	28
8.2.3	Searching for LLPs	28
8.2.4	The Search for LLCPs	29
9	Conclusion	31

Appendices	33
A Engineering Change Request	33
B Safety Derogation Request	46
C List of parts for the Phase-1 MAPP detector (MAPP-mQP)	52

1. Introduction

The discovery of the Higgs boson announced in 2012 by the LHC’s large general purpose detectors (GPDs), ATLAS and CMS, put in place the last piece of the Standard Model (SM) puzzle. Unfortunately, evidence for physics beyond the Standard Model is still not forthcoming at the LHC. A logical possibility is that conventional collider detectors are not optimized to detect the new physics present. MoEDAL is the first of a series of “dedicated experiments” [1] planned for the LHC that is designed to provide a complementary coverage for Highly Ionizing Particle (HIP) messengers of physics beyond the SM at the LHC. The MoEDAL-MAPP experiment for Run-3 extends this complementarity to include weakly ionizing particle (eg milli-charged particles or mCPs), very Long-Lived Charged Particle (LLCPs) and very Long-Lived weakly interacting neutral Particle (LLPs) avatars of new physics.

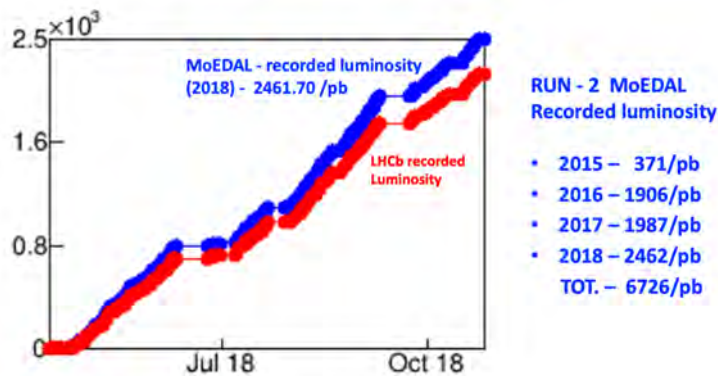


Figure 1: The luminosity recorded by MoEDAL during Run-2.

MoEDAL officially started data taking in 2015 at a centre-of-mass energy (E_{CM}) of 13 TeV and operated with 100% efficiency during LHC’s Run-2, receiving 6.7 fb^{-1} of data, as shown in Figure 1, well short of the 10 fb^{-1} requested. Although the analysis of this data will continue through the LHC long shutdown (LS2) we have already placed the world’s best limits on singly and multiply charged monopole production via the Drell-Yan (DY) mechanism, using detector technology that is directly sensitive to the magnetic charge of the monopole. Importantly, MoEDAL has expanded the search to include monopole production via photon-fusion, for the first time at the LHC. Additionally, the search for: spin-1 monopoles; dyons; and monopole production in heavy-ion collisions via the Schwinger Mechanism was carried out for the first time, ever. The results of the ATLAS and MoEDAL searches for the monopole are [2, 3, 4, 5, 6, 7, 8, 9].

Searches for massive singly electrically charged objects from a number of new physics scenarios involving, for example, supersymmetry and extra dimensions, described in MoEDAL’s published physics program [10], are also underway. For example, a MoEDAL team of theorists and experimentalists has shown that we could make significant contributions to the search for SUSY using the enhanced luminosity of LHC’s Run-3 [11].

A major part of the MoEDAL Collaboration’s physics program for LHC’s Run-3 and beyond involves the installation of a new detector called MAPP (MoEDAL Apparatus for Penetrating Particles). A current plan of the LHC’s future program is shown in Figure 2. MAPP’s purpose is to expand the physics reach of MoEDAL to include the search for mini-charged particles¹ (mQPs) with charges as low as one thousandth the electron charge (e) and weakly

¹We use the term mini-charged rather than milli-charged to denote the lightly ionizing particle as it does not imply that the charge is $10^{-3}e$

interacting very long-lived neutral particle (LLPs) messengers of new physics. Thus the MoEDAL and MAPP detectors operating together will be able to detect: HIPs, mCPs and LLPs. The MAPP-mQP detector can also be used to monitor exposed trapping volumes from MoEDAL’s MMT detector placed underneath the MAPP-mQP detector for the decays of captured LLCs. We can rapidly transfer MoEDAL’s exposed trapping detectors underground to the MAPP-mCP detector in UA83, in order to maximize the range of lifetimes to which this arrangement is sensitive.

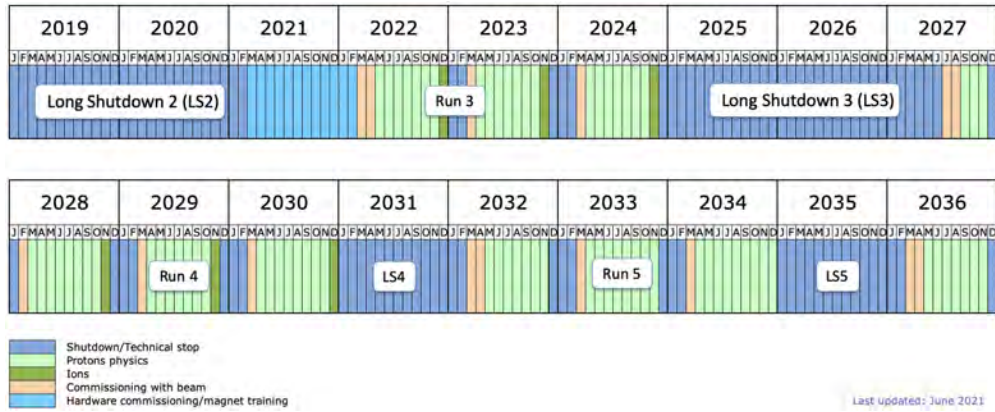
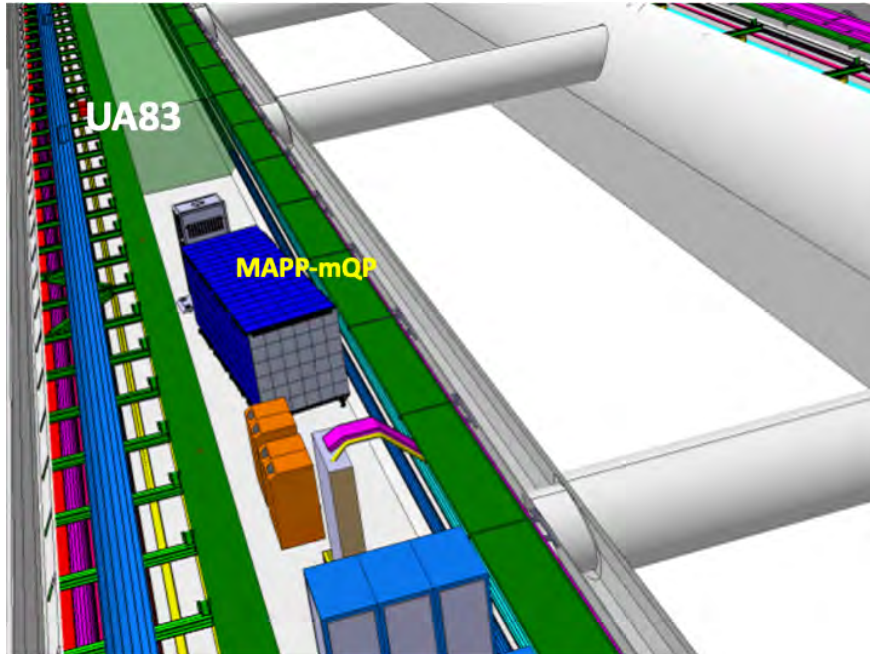


Figure 2: A overview of the full LHC program up to and including HL-LHC.

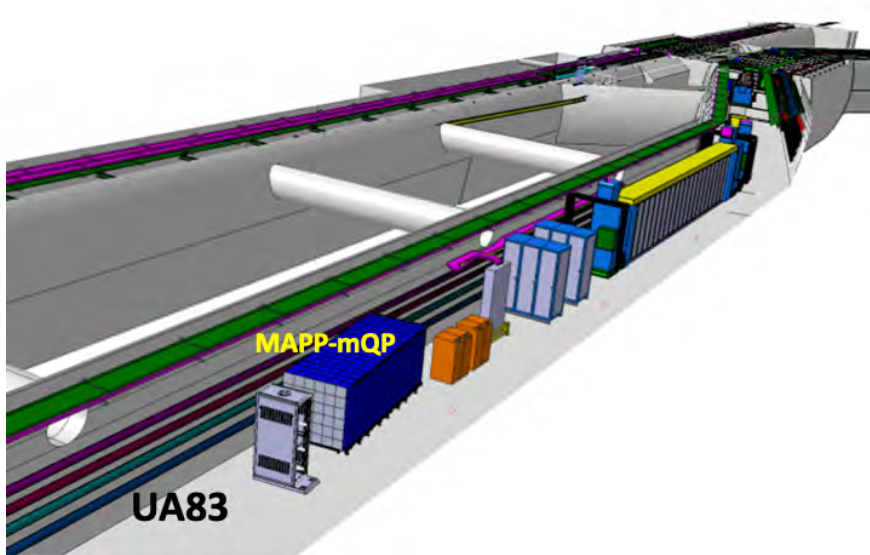
In February 2020 the MAPP-mCP detector was first presented to the LHCC as a MoEDAL upgrade for Run-3, as Phase-1 of a broader upgrade plan encompassing Run-3 and HL-LHC. At this time the deployment of the MAPP-mCP detector was planned for the UGC1 gallery, at a position 55m from IP8 at an angle of 6.5° to the beam axis. At this position the MAPP-mCP detector would be protected by roughly 25m of rock from Standard Model (SM) backgrounds and cosmic ray backgrounds by a 110m rock overburden. A prototype detector was deployed in UGC1 in 2018 to assess cosmic ray and beam related backgrounds.

However, the UGC1 gallery is not commissioned as an experimental area. Subsequently, a safety review of the UGC1 gallery revealed a number of access and safety issues that required extensive modifications and upgrades to remedy , including roughly 6 months of civil engineering work. Although the MoEDAL Collaboration had sufficient funding to complete the work there was not sufficient time to finish it before the start of Run-3. An alternate location for the MAPP-mCP in the UA83 tunnel was suggested in June 2021. This new position is already a full part of the LHC infrastructure with direct elevator access, with the required access interlocks and safety measures in place. The adoption of the UA83 tunnel as the new home of the MAPP-mCP detector, is described in ECR (LHC-X8MAPP-EC-001) a copy of which is included in Appendix-A. Final approval of this document was obtained from the LHC Machine Committee in November 2021.

The MAPP detector will be deployed in two phases each of which will have its own Technical Proposal (TP). Phase-1, the subject of this TP, will see the installation of the MAPP-mCP detector (MAPP-1) in the UA83 gallery, adjacent to IP8. The Phase-1 detector will be installed for data taking in Run-3. Phase-2, involving the additional installation of a MAPP-2 in the UGC1 gallery - where the fiducial volume in which to detect decays-in-flight is much larger - is planned for High Luminosity LHC (HL-LHC) running, starting in 2027 (Run-4).



(a)



(b)

Figure 3: The deployment of the MAPP-mQP detector in UA83.

2. The Phase-1 MAPP-mCP Upgrade

The Phase -1 MAPP-mCP upgrade will be installed in UA83 tunnel some 100 m from the existing MoEDAL/ LHCb detectors, in order to take data during LHC's Run-3. A complete GEANT4 description of MoEDAL, MAPP, and the adjacent and intervening volumes is nearing completion. The MAPP-mQP detector and its associated electronics rack has now been included in the overall LHC machine description as shown in Figure 3. A detailed engineering drawing of the MAPP-mCP detector is shown in Figure 4. MAPP-mCP is protected from Standard Model particles from interactions at IP8 by roughly 35m of rock and from cosmic rays by an overburden of approximately 110m of limestone.

2.1. The MAPP - mCP Detector

The MAPP Phase-1 detector is dedicated to the search for mCPs. It is made up of four collinear sections, with sensitive cross-sectional area of 1.0 m^2 , each comprised of 100 ($10 \text{ cm} \times 10 \text{ cm}$) plastic scintillator bars each 75cm long. A drawing of this basic subunit of the MAPP-mQP detector is shown in Figure 5. Each bar is readout by one low noise 3-inch PMT. The detector is arranged to point towards the IP. Thus, each through-going particle from the IP will encounter 3.0 m of scintillator and be registered by a coincidence of 4 PMTs. The 4-fold PMT coincidence essentially eliminates the background from "dark counts" in the PMTs. Additionally, the division of the detector into 4 bars virtually excludes all fake 4-fold coincidences due to radiogenic backgrounds in the scintillator and PMTs.

The MAPP-mCP "bar" detector is hermetically enclosed in a veto layer consisting of 1cm thick scintillator read out by embedded scintillating fibre loops with a pitch of $25 \text{ cm} \times 25 \text{ cm}$.

The final design of the MAPP-mCP was refined with the help of studies of a prototype detector deployed in the UGCI gallery that took place during 2018. The prototype consisted of nine 2m long bars with cross-section $10 \text{ cm} \times 10 \text{ cm}$, arranged in a 3×3 configuration. A photograph of the prototype detector and the readout electronics is shown in Figure 6.

2.1.1. MAPP- mCP Mechanics

As can be seen in Figure 4, the MAPP mechanics is divided into 4 sub-sections, where each sub-section corresponds to an array of 100 scintillator bars. The main support structure is comprised of generic T-bar extruded aluminium construction bars, a cross-section of such a bar is shown in Figure 7. Each leg of the support structure is adjustable, in order that the height of the structure can be adjusted to ensure the detector is pointing to IP8.

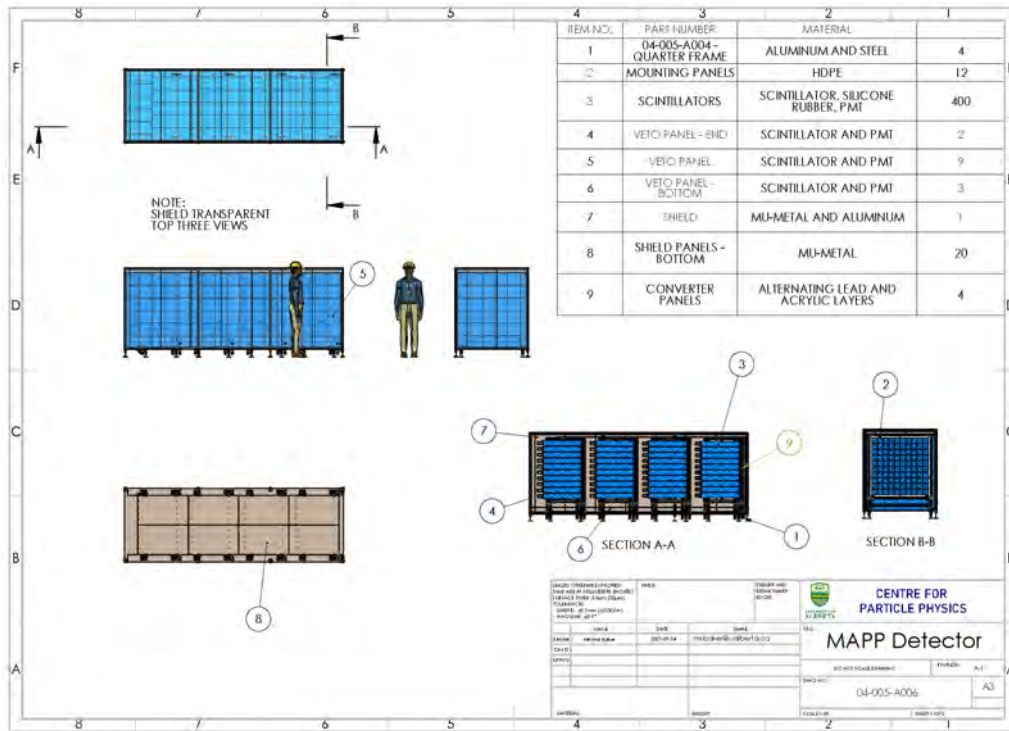
The scintillator bars in each of the four sections of the MoEDAL-mQP detector are supported by three matrices machined out of 1" thick high-density polyethylene (HDPE) plate, making twelve supports in all. These matrices are slotted into the T-bar support structure, as shown in Figure 4. The complete structure is made to be assembled from scratch from component parts weighing less than 20 kg. Once the mechanical support structure is assembled and surveyed-in, the scintillator bars with the PMTs attached will be loaded into the HDP matrix, which is constructed in order to ensure that the scintillator bars are aligned and point to IP8.

2.1.2. The MAPP-mQP Calibration System

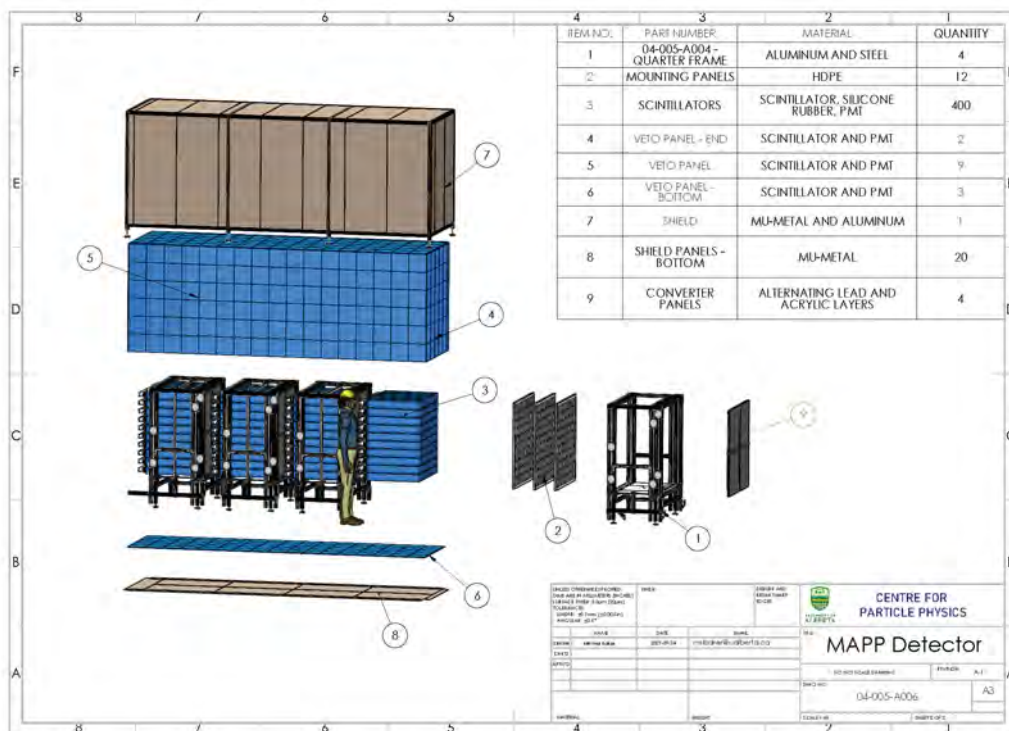
The MAPP-mQP detector will be calibrated in two main ways. The first method utilizes an array of blue LED's emitting at the peak of the wavelength sensitivity of the scintillator bars forming the MAPP-mQP detector. Each scintillator bar is equipped with a LED which is pulsed in such a way as to mimic the light deposited by particles with varying fractional charge, down to the level where only single photoelectrons are being detected by the PMTs. A sketch of the LED calibration array for one of the four sections of scintillator bars is shown in Figure 8.

The second calibration method employs the small flux of high momentum muons from IP8. Characteristically, these muons will be minimum ionizing particles (MIPs). Typically, they will lose 2 MeV/cm in the plastic scintillator and generate of the order of 10,000 photons per MeV lost. Consequently, muons will deposit a comparatively large amount of light, of the order 6×10^6 photons in the 4 consecutive scintillator bars through which the muon passes. We have estimated that the light collection efficiency, including the loss due to photocathode efficiency, is 5%. As a relativistic charged particle ionizes according to the square of its charge a particle with charge a few times $10^{-3} e$ will give of-the-order-of a single photon in each bar.

We can simulate the light emission of a fractionally charged particle by inserting a neutral density filter between the PMT and the scintillator bar. The transmittance of the filter would be chosen to reduce the amount of light entering the



(a)



(b)

Figure 4: An engineering drawing showing a 2D (a) and a 3D (b) exploded view of the mechanics and composition of the MAPP-mQP detector.

ITEM NO.	PART NUMBER	WEIGHT (KG)	QTY.
1	Scintillator Body	7.73	1
2	PMT Cover	0.08	1
3	Light Guide	0.24	1
4	PMT	0.71	1

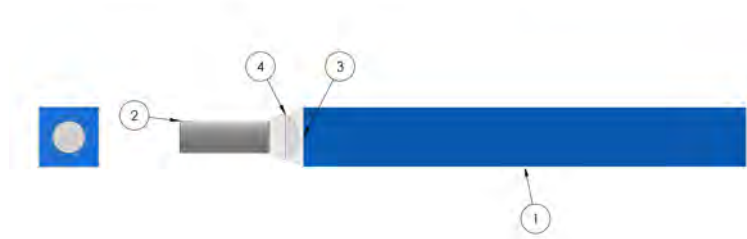


Figure 5: A drawing, to scale, of MAPP-mQP scintillator bar subunit



Figure 6: A photograph of the prototype MAPP-mQP detector and its readout system deployed in the UG1 gallery near to IP8

PMT from the muon by the same amount that a fractionally charged particle would have reduced ionization compared to a MIP. This "absolute" calibration is transferred to the LED system by comparison of the signal generated by the calibration LED in the PMT to the signal obtained when a neutral density filter is interposed.

We will perform studies in the lab. with cosmic ray muons using scintillator bars equipped with filters and LEDs. This will enable us to be able to transfer the calibration using filters, to the LEDs. This "pre-calibration" will be carried out on 25% of the bars using a cosmic ray coincidence units that allows us to test 4 bars at a time. Test will be performed with the bars placed vertically and with the bars placed horizontally. The pretested bars will be placed as the top layer of each section. During the run vertical cosmic rays that traverse the cosmic ray veto and all layers of scintillator will be recorded. In these events pre-calibrated bars would be included in each recorded event. In this way we can cross-calibrate all bars using cosmic rays during the run in a way that can be checked with pre-calibrated bars. This process is included in the resource loaded spread sheet.

We aim to have a small number of bars equipped with filters during data taking in order to check the calibration over time using muons from the interaction point. The filters can be moved/removed manually during shutdowns. Calibration transfer studies will be carried out using neutral density filters corresponding to particles with several different mini-charges, down to a charge of 0.001e. We expect to be able to be interpolate between these points to obtain an understanding of the calibration across the sensitive range, using the LEDs. The daily LED calibration will

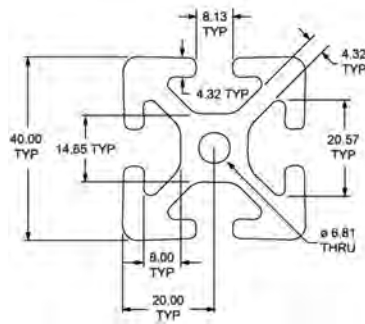


Figure 7: A picture of a section of the T-slot extruded aluminium support bar used to create the main load bearing members. All dimensions are in millimetres.

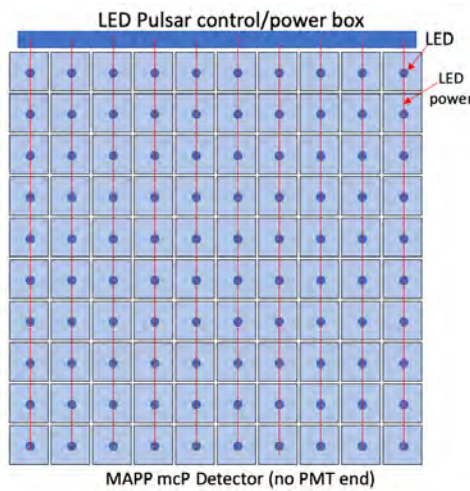


Figure 8: A sketch of the LED calibration system for one of the four sections of MAPP-mQP scintillator bars.

be performed with a number of different pulse times and voltages corresponding to particles with different ionizations.

2.1.3. The MAPP-mQP Veto System

The MAPP-mQP detector is hermetically encased in a scintillator veto layer as shown in Figure 9. The veto layer consists of scintillator tiles of size 25cm x 25cm and thickness 1cm. We will readout the tiles using 2 embedded wavelength shifting fibres (WLS) of diameter 1mm readout by a SiPM (KETEK PM3225WB 3 x 3 mm²), as shown in the Figure 10.

Our GEANT simulations show that efficiency is 99.7% - 100% in the centre with only small drops at the edges to 99.5% - 99.7% at worst. This is consistent with beam tests of a similar tile (30 cm x 30 cm x 0.5 cm with 2 fibres and a 3 x 3 mm² SiPM) [12]. Note also that, due to the geometry of the veto system, any through-going particle would give a signal in two veto tiles as well as the detector bars. Thus, it will be possible to monitor the efficiency of the veto tiles.

We can also monitor the performance of the CR veto system of the MAPP-mCP detector during data-taking and also when the beam is off. In the event that more VETO power is required we can utilize the outer layer of 10 cm x 10cm scintillator bars as an additional VETO layer. As we have a software trigger we can change existing VETO conditions and if necessary implement the extra VETO power offline using the recorded data.

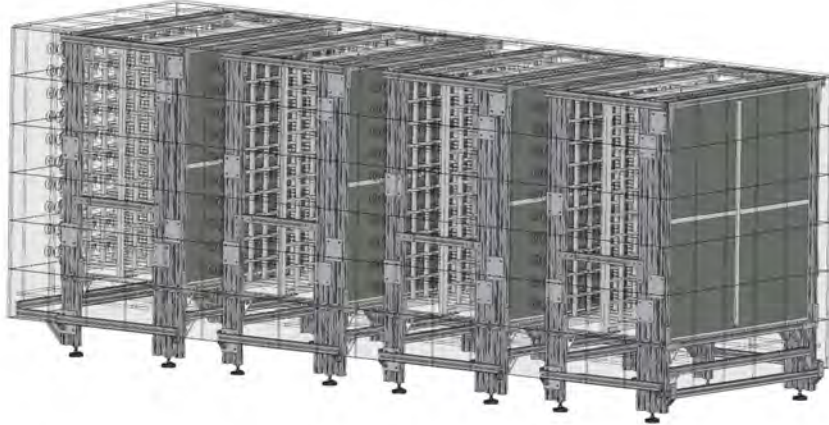


Figure 9: A drawing of the MAPP-mQP veto system.

2.1.4. MAPP-mQP Radiator Layers

A radiator layer, the purpose of which is to tag electrons and photons, is placed at the front of the MoEDAL-mQP detector and in between each of the scintillator sections 1 & 2, 2 & 3, and 3 & 4. Each of these layers consists of five 2 mm layers of lead interleaved with 5 mm layers of plastic scintillator, readout at the edge by wavelength shifter bars connected to SiPMs. Each radiator layer is two radiation lengths thick. An engineering drawing showing the deployment of the radiator layer in one section of the MAPP-mQP detector is shown in Figure 11. The radiator layer is divided into four parts so that each part weighs less than 100kg. The purpose of the radiator layers is to tag photons and electrons.

However, if there is some indication of BSM physics involving long-lived particles resulting in photons or electrons, we envisage equipping the front of MAPP-mQP with Shashlik-type calorimeters with dimensions of 20cm x 20cm x 75cm long (25 radiation lengths) comprised of 70 layers of lead/scintillator, where the scintillation light is readout by wavelength shifting fibres, into SiPMs. The Shashlik calorimeters with a total depth of 25-30 radiation lengths, would be similar in design to those used in HERA-B and LHCb [13]. Such an arrangement allows ~1% energy resolution for 1 TeV electrons.

2.1.5. MAPP-mQP Frontend, HV, DAQ and Trigger

The PMT used in the readout of the scintillator bars is a HZC Photonics ZP72B20 PMT Tube. The High Voltage divider will be resistive with an impedance of $4M\Omega$ a maximum voltage of 2000V and a current of $500\mu A$. The photocathode will be at ground potential with positive high voltage applied to the anode. The signal will be capacitively coupled to the cable.

The power supply will consist of a boost converter to convert from 48Vdc to 250V using a coupled inductor to reduce the maximum voltage seen by the controller. Several stages of a Cockcroft-Walton multiplier will then increase this up to 2000V. The boost converter will be controlled by a small inexpensive 6 pin micro-controller which can accept serial data and synchronization pulses from the DAQ. The Front end is connected to the DAQ via an MCX connector. Power, signal and control will all be delivered via the same cable to reduce cabling costs. In this way we avoid HV cables and connectors as well as the related safety concerns.

A block diagram of the electronic readout and powering scheme is shown in Figure 12. Each DAQ board will consist of 32 identical channels. The DAQ will connect to the front end via an MCX connector. A bias tee will couple the 48V dc supply to the signal line. Control signals for the high voltage power supply will also be coupled capacitively to the signal line. The amplifier chain will include a programmable gain amplifier to allow tuning of the overall system gain, minimal shaping and an anti-alias filter. The ADC will consist of a Texas Instruments ADS4249 dual channel amplifier running at 240MHz, and 14bit readout to an Intel (formally Altera) Cyclone IV FPGA via LVDS.

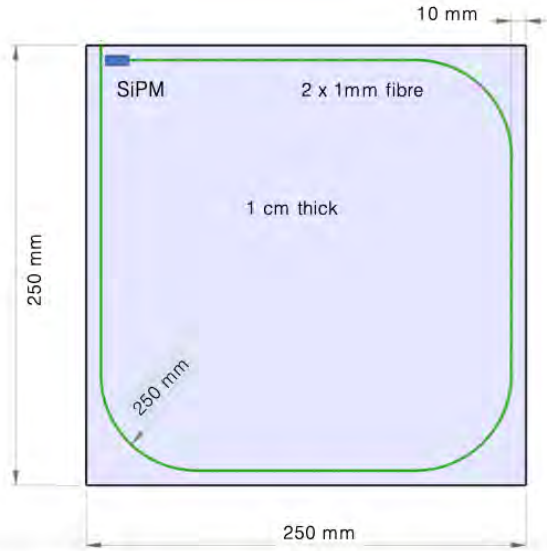


Figure 10: A drawing of a scintillator tile readout by WLS fibres that comprises the MAPP-mQP veto system.

The FPGA will perform discrimination, coincidence and peak detection of the incoming signals, with inter-fpga communication via backplane B-LVDS. Events that pass both the software trigger and the veto will be passed for storage via Ethernet to the PC(s). The system will run synchronously to the LHC (bunch crossing) clock, The orbit clock will also be veto background events from non-colliding bunches and to synchronize health keeping events and switching regulator noise to the abort gap.

Normally the data will be transferred via 1 Gbit/s ethernet link to an external computer. There will also be a computer in UGC1 that will take data if there is a failure in the ethernet connection. The data will be sent via the onsite storage via the internet to analysis sites in Canada, UK, USA, Spain and Italy. The 19 readout boards will be housed directly underneath the MAPP-mQP detector, in the UGC1 gallery.

The data rate is expected to be on average less than 1 Hz from each of the 400 bars of the main detector with around another 200 channels from the veto detectors and radiator at maximum. In addition, conservatively assuming a rate of, on average, 1 Hz for each channel with 200 bits per channel (or PMT pulse) being readout, our system has the capacity to readout 4 million channels/s, 7000 times more capacity than needed. The data in the frontend readout electronics is pipelined, so that large fluctuations up in the data rate can be handled. Thus, these boards could be used for high luminosity LHC.

There will be a number of software triggers carried out by FPGAs housed in the readout system. The trigger philosophy is to widen the trigger as much as possible. Additionally, we aim to take minimum bias events at the rate of approximately 5% of the total data rate. Nevertheless, we expect the amount of data readout will be somewhat less than the maximum mentioned just above. Further, higher level “triggers”, will be applied offline to the raw data. We chose to adopt the philosophy of utilizing a very broad software trigger, rather than reading out the complete detector at each beam crossing, since the flow of data through the various triggers enables us to monitor the physics response of our detector online.

An example of an important “software” trigger for MAPP-mQP is the through going muon-trigger. In this case the muon would pass through all four scintillator bars pointing at the IP (note that the MAPP-mQP detector has a pointing geometry) as well as the photon tagging boards (that can also serve as VETO detectors) that sandwich the main scintillator detector sections. In this case a basic muon trigger is formed from a coincidence of 4 contiguous scintillator sections as well as a signal in the scintillators of the photon tagging detectors. We expect this trigger efficiency to be very near 100%. We can refine the basic muon trigger by, for example, additionally demanding no hits in the surrounding VETO detectors. The trigger for a mini-charged particle would include all the elements of this muon trigger but instead use the photon tagging detectors as a veto.

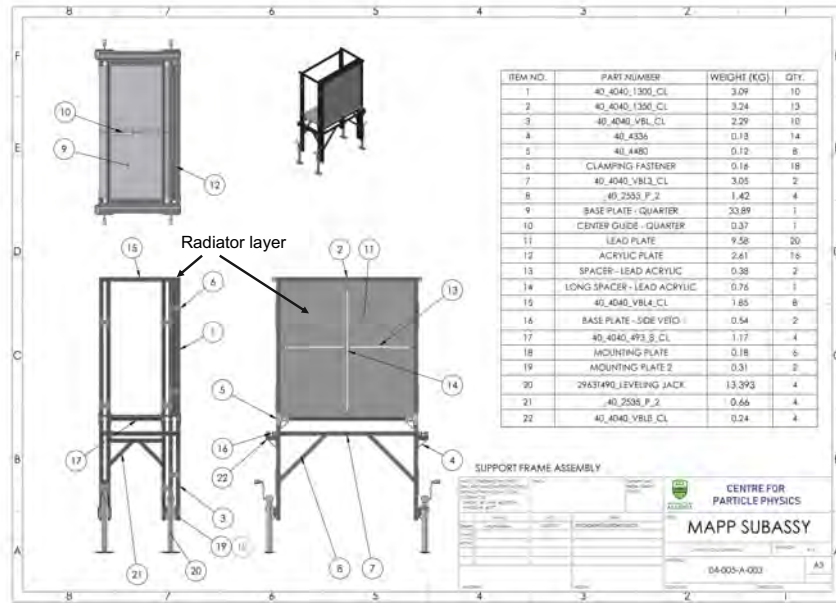


Figure 11: An engineering drawing showing the deployment of a radiator layer in one section of the MAPP-mQP detector.

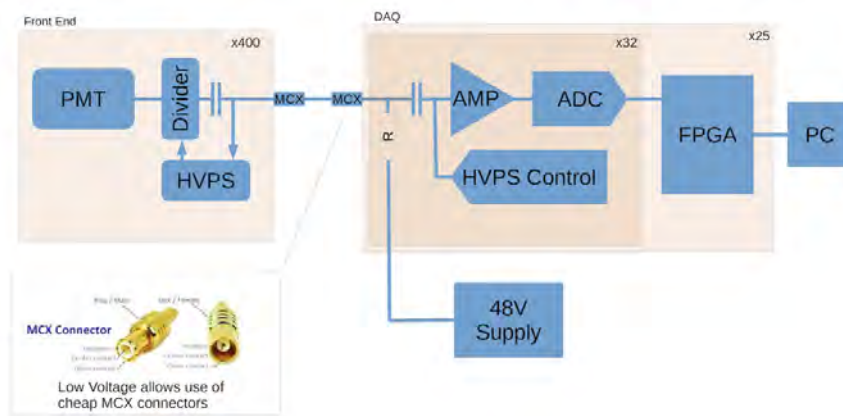


Figure 12: A block diagram showing the basic electronics readout structure for the MAPP-mQP detector.

3. The MAPP-mCP Deployment in the UA83 Tunnel

The possibility of the deployment of the MoEDAL-mCP detector in the UA83 tunnel in the region of IP8 on the LHC ring was first suggested in June 2021. It is now the proposed position for MAPP-mCP. A photograph of the UA83 tunnel with the envelope of the deployment position marked is shown in Figure 13

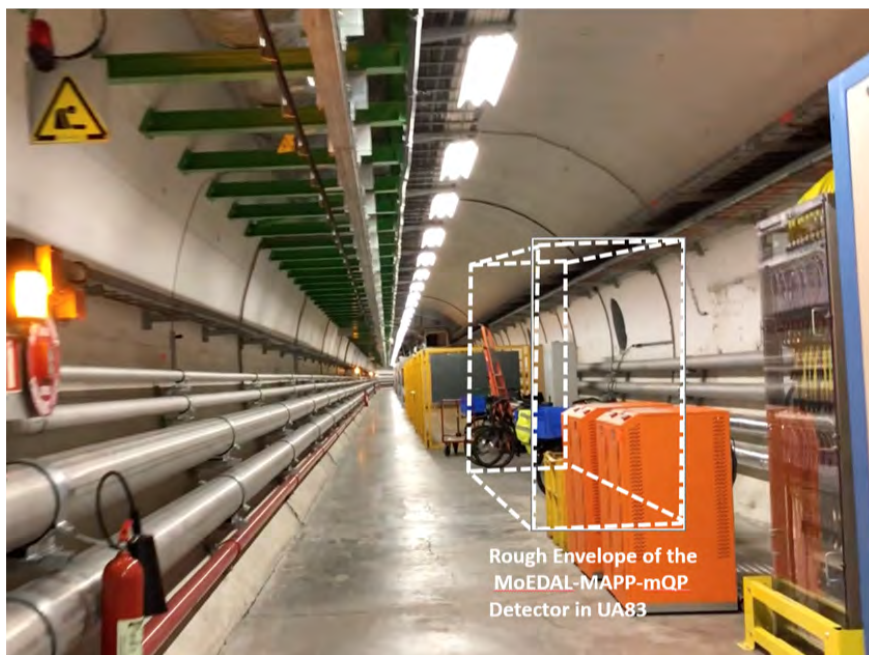


Figure 13: The position envelope of the MAPP-mCP detector in the UA83 tunnel.

As discussed in the ECR and the section on Safety Matters below, the UA83 location solves all of the safety concerns related to the detector's placement.

3.1. Staging and Temporary Storage Area

In order to facilitate the installation and operation of the MAPP-mCP detector, the LHC machine side manager responsible for allocation of surface space in the SBD building agreed that MoEDAL-MAPP Experiment can be temporarily attributed about 20 m² of surface space in SBD 2855, as indicated in the photograph in Figure 14. This area will be used as buffer space for short term storage of equipment before transport and installation underground, and for storing light tooling needed for assembly and installation. The zone will be cleared and fenced with mobile barriers and will be made available to the collaboration as of week-46 of 2021.

3.2. Beam Induced Radiation Backgrounds in the MAPP-mCP Region of the UA83 Tunnel

Francesco Cerutti and Alessia Ciccotelli of the Beam-Machine Interaction section of the CERN Engineering Department have performed a study of the beam induced backgrounds in the UA83 tunnel and the UGC1 gallery using the FLUKA Monte Carlo program, assuming an annual luminosity of 10 fb⁻¹. A critical issue is the affect of the radiation on the detector and on its electronic readout system. A key variable here is the dose which is shown in Figure 15. As can be seen from Figure 15 the dose received by the MAPP-mCP detector in its the new position in the UA83 tunnel is estimated to be below 1mGy/year, a factor of 300 less than its initially proposed deployment in the UGC1 gallery.

Figure 16 shows a map of the muon fluence component of beam induced backgrounds expected at the UA83 (< 10⁶ cm⁻²) and UGC1 (~3 × 10⁸ cm⁻²) locations of the MAPP-mCP detector. We see a better than a 300 times reduction of the muon flux in the UA83 location compared to the UGC1 position.



Figure 14: The temporary staging area in SBD 2855.

Likewise the neutron flux ($5 \times 10^7/\text{year}$) and photon flux ($10^8 \text{ cm}^{-2}/\text{year}$) at the position of the MAPP-mCP detector in UA83 show at least a few hundred time reduction over MAPP-mCP's previously proposed position in the UGC1 gallery, as shown in Figure 17 and Fig 18, respectively.

3.3. Beam Induced Backgrounds in the MAPP-mCP detector in UA83

A prototype MAPP-mQP detector was deployed during 2018. Its main purpose was to enable us to estimate the data rate we would expect during RUN-3. The prototype was comprised of nine $10 \text{ cm} \times 10 \text{ cm} \times 120 \text{ cm}$ scintillator bars deployed in a *horizontal* configuration in the UGC1 gallery, as shown in Figure 6. Each bar was readout at both ends by a PMT. A hit on a scintillator bar was counted if the PMTs at each end of the bar registered a coincident signal above threshold. We observed that with beam-off each bar was hit at around a rate 0.05 Hz . We assumed that this rate was largely due to cosmic rays, despite the 100m rock overburden. This level of cosmic background was consistent with our GEANT-4 based simulations.

By comparison, the CODEX-b collaboration measured rates [14] of 10^{-3} Hz in the main cavern with *vertically* deployed $30 \text{ cm} \times 30 \text{ cm}$ scintillator sheets. Considering the deployment and size of the test detectors and the slightly greater overburden in the UGC1 cavern we feel our measurements are compatible with CODEX-b's.

When the beam was on we observed the rate in the MAPP-mQP prototype bars increased by a factor of 4 to 5. The CODEX-b measurements indicated an increase of around a factor of ~ 30 adjacent to LHCb at the most upstream measurement point, to ~ 500 at the most downstream monitoring point in the main cavern. We consider the two main reasons for this difference are as follows:

- The MAPP-mQP prototype was deployed $\sim 55\text{m}$ upstream of the collision point in a tunnel largely surrounded by rock and far from the flux of secondary particles scattered by elements of the LHCb detector;
- The MAPP-mQP is protected by over 26m of rock and beam line elements from the IP. Whereas, the CODEX-b scintillators were only protected by a 3.2m thick concrete wall.

According to the FLUKA studies presented in the above subsection on beam induced radiation backgrounds in the MAPP-mCP region of the UA83 tunnel, the beam induced backgrounds in the MAPP-mCP detector in UA83 should be considerably less than expected in UGC1. Background from cosmic ray that penetrate to the overburden should be roughly the same as that expected in UGC1.

Dose

Annual luminosity 10 fb^{-1}

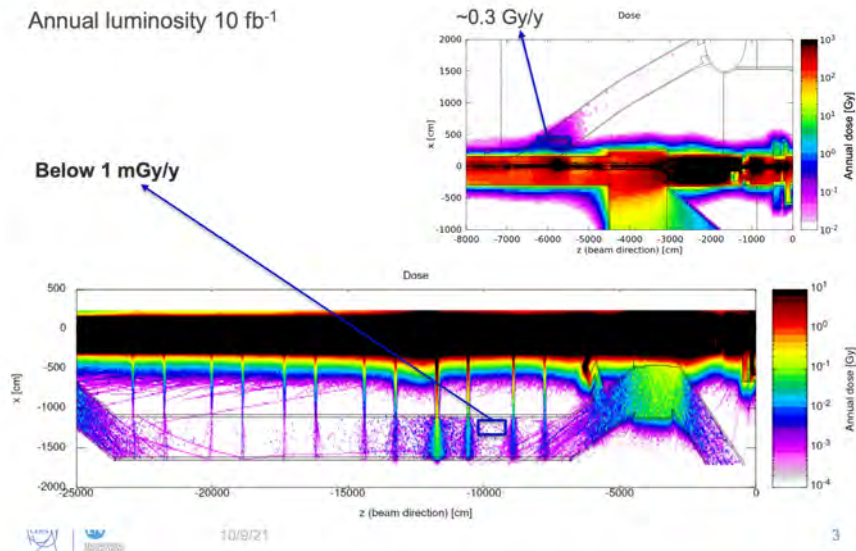


Figure 15: The dose rate in the vicinity of MAPP-1. The top map shows the UGC1 gallery and the bottom map shows the UA83 tunnel.

3.4. Installation of Required Infrastructure

The MAPP-mCP detector will require some additional infrastructure to be installed in UA83 for meet operational and safety requirements. The installed item and installation schedule are given in the itemized list below:

- One electronics rack with cable trays connecting to tunnel cable tray - Ticket: RQF1906969, to be installed in December 2021;
- 5 x 16 AMP socket (or two 10 AMP sockets) with dedicated AUL to be installed close to the detector - Ticket: RQF1836639 (EN-EL-EWS), installed in the winter of 2021;
- 1 x optical fibres carrying the LHC beam orbit clock, to be pulled from rack CYFIB01 in UA83, shown in Figure 19, to the MAPP-mCP detector electronics rack in UA83 - Ticket: RQF1801156 (EN-EL-FO), to be installed in December 2021;
- Feed for CERN Control Centre - to be installed and tested prior to power on of MAPP-mCP detector in January 2022:
 - 6 x Temperature sensor signals from sensors on MAPP-mCP flame shield;
 - Current and voltage readings from MAPP-mCP power supplies
 - Feed from IR camera deployed in the area, looking at the MAPP-mCP detector and electronics rack.

Muon fluence

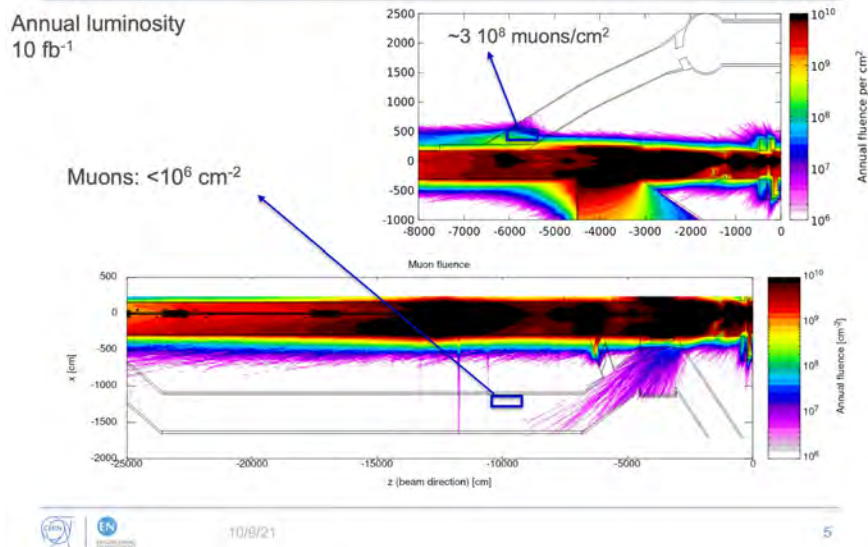
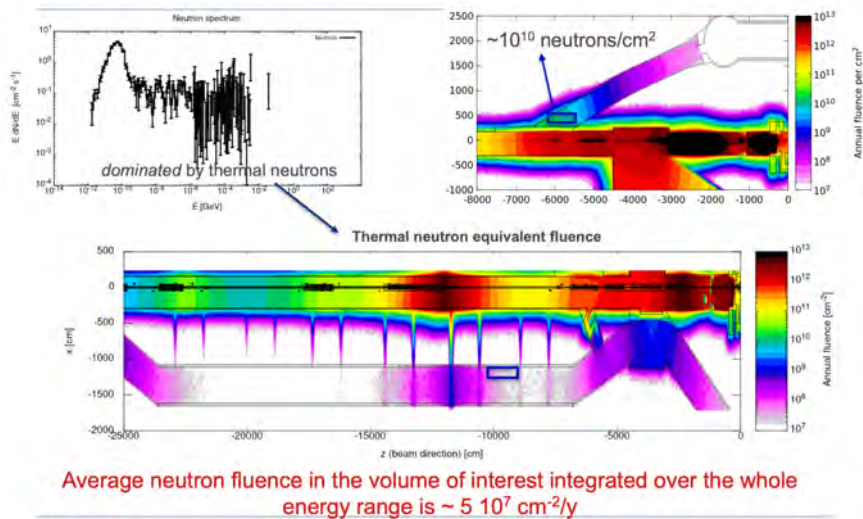


Figure 16: The muon fluence in the vicinity of MAPP-1. The top map shows the UGC1 gallery and the bottom map shows the UA83 tunnel.

Neutron fluence



htb]

Figure 17: The neutron fluence in the vicinity of MAPP-1. The top map shows the UGC1 gallery and the bottom map shows the UA83 tunnel.

Photon fluence

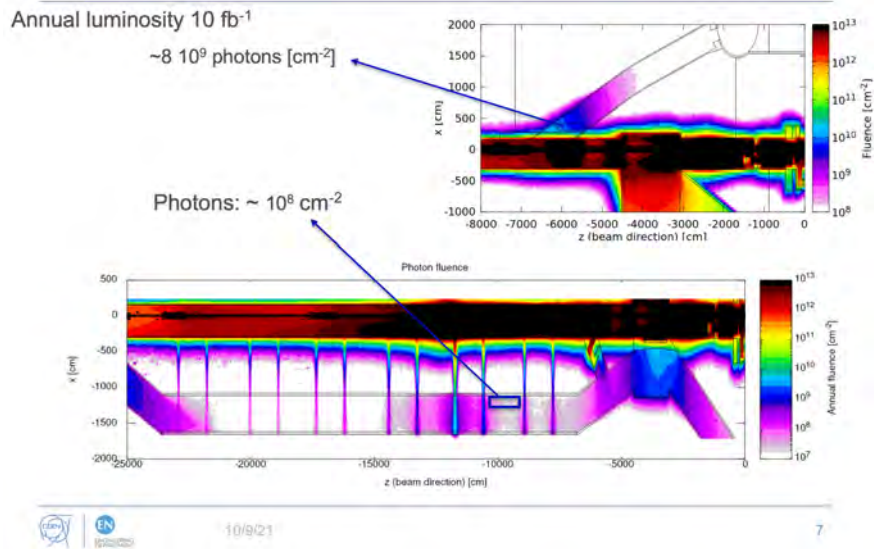


Figure 18: The photon fluence in the vicinity of MAPP-1. The top map shows the UG1 gallery and the bottom map shows the UA83 tunnel.



Figure 19: The source of the optical fibres carrying the LHC clock to the MAPP-mCP detector.

4. Safety Matters

The safety issues considered below arise from four sources, those to do with: the UA83 tunnel; the detector itself; and, detector operations.

4.1. UA83 Tunnel Safety Issues

The UA83 tunnel is a full part of the LHC machine infrastructure with access via the PM85 lift directly to the floor of UA83. It is equipped with interlock access, smoke detector, fire alarms and forced ventilation. It does not suffer from the safety and access problems that were present in the MAPP-mCP detector's previously planned position in the UGC1 gallery [15, 16].

The remaining safety requirements arise from the detector's deployment in UA83 tunnel are related to the positioning of the detector within the tunnel. In order to meet these requirements the MAPP-mCP was placed directly adjacent to the wall closest to the beam-tunnel outside of the area delineated for tunnel access. In addition, the detector was placed 1.5 m away from the nearest active element of the LHC infrastructure (rechargeable power supplies).

4.2. Safety Issues Relating to the MAPP-mCP Detector

The MAPP-mQP employs conventional detector technology involving scintillator detectors and electronic readout, no gaseous detectors are involved. The safety issues directly related to the MAPP-mCP detector are presented in an approved Safety Derogation Request (SDR) [19] and described directly below. The SDR is included in Appendix (B).

4.2.1. Readout Electronics and HV

The readout electronics is isolated and deployed some 1.5 m from the detector. There are no HV cables or connectors as there is a "Cockcroft-Walton" type converter in the base of each PMT that converts LV power to HV power for the PMT. The power supplies are low voltage (24V), are current and temperature limited (turn off when current or temperature goes out of a predetermined range) and provide an alarm signal when current or voltage moves out of some predefined operating window.

All cabling is halogen free according to the provisions in IS23². The only heat source in the UGC1 gallery arises from the MAPP-mQP detector electronics and amounts only 1200 watts.

4.2.2. The Scintillator Detectors and Their Support Structure

The MAPP detector is comprised of 400 x (10 cm x 10 cm x 75 cm) scintillator bars weighing 3 T. All bars are wrapped in Tyvek and then black tape and connected via a short light guide to a 3-inch PMT. The bars are arranged in 4 sections, each with 100 bars with overall sensitive area of 1m². The scintillator bars (NUVIA polystyrene based scintillator) in each section are held in a square array by three support grids made of High-Density Polyethylene (HDPE). A drawing of one of the basic HDPE support grids is shown in Figure 20. The grid separates the bars one from the other by 5 to 7 mm. Air fills the interstices between the scintillator bars. The HDPE support structures are emphasized in Figure 9. HDPE has been used extensively at the LHC. For example, in the shielding of the ATLAS Forward Region³ Polystyrene based scintillators were used for the ATLAS Hadronic Tile Calorimeter⁴ and also the LHCb SciFi tracker uses fibres with a polystyrene core⁵

The weight of the scintillator in each section is supported by an aluminium T-bar support structure and a 0.5 cm aluminium plate that forms the base of each section. Additionally, each section is protected from the other by the lead-scintillator radiator plane that includes 2 x 1 mm of aluminium sheet and 5 x 2mm layers of lead. The active detector is completely encapsulated in VETO detectors comprised of 1 cm thick acrylic scintillator (Eljen-200 PVT based scintillator) with area roughly 30m² and mass approximately 0.3 T. The arrangement of the metal plates and radiator layers is shown in Figure 11.

²<https://edms.cern.ch/document/335745/4>

³<http://cds.cern.ch/record/683739/files/tech-98-033.pdf>

⁴ <https://cds.cern.ch/record/1075711/files/cer-002731189.pdf>

⁵<https://arxiv.org/abs/1710.08325>

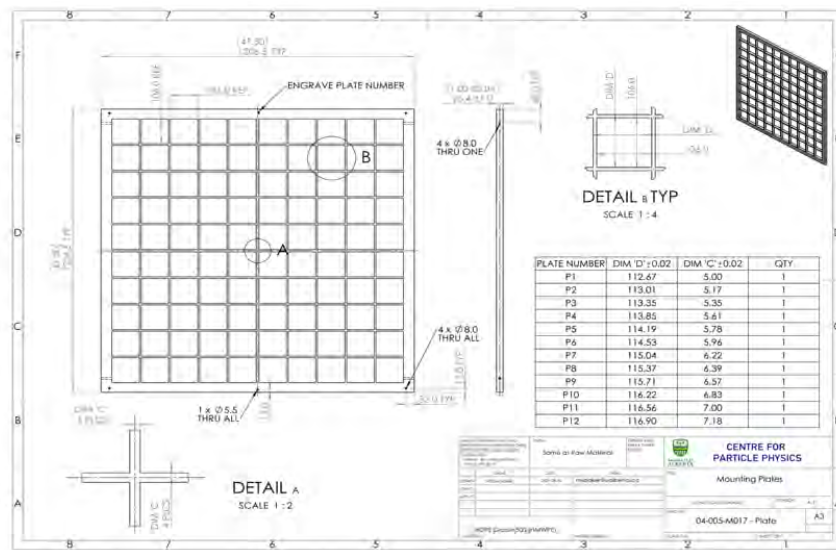


Figure 20: A drawing of one of 12 HDPE support grids of the MAPP-mQP detector.

The veto counter scintillators are comprised of PVT based plastic scintillator. Examples of other LHC/LEP uses of PVT based scintillators are the beam scintillation counters for CMS ⁶ and LHCf's Scintillator detectors⁷.

4.2.2.1. The Flame Shield. The MAPP detector and VETO layer are completely enclosed in an aluminium flame shield as shown in Figure 21. The size of the shield is roughly 1.3m x 1.5 m x 4m. The flame-shield is fabricated out of 1mm thick aluminium sheet and has a total area of ~30 m². The aluminium enclose the plastic scintillator completely. There is no break in the flame shield for cable exit. The cables exit via a patch panel.

In order to provide a hermetic environment all joints in the flame shield are sealed using heavy duty aluminium tape. Any fires within the flame shield volume would be suppressed due to lack of oxygen. The slight electrical heating arising from the PMT bases within the volume of the flame shield the only electrical elements in the region - amounts to a few hundred Watts that is dissipated by conduction and radiation from the flame shield surface.

4.2.3. Presence of Lead in the Radiator Layers

The only lead that we planning at present deploy is in the radiator layers of the MAPP detector. The lead is placed at the front of the MoEDAL-mQP detector and in between each of the scintillator sections 1 & 2, 2 & 3, and 3 & 4. Each of these layers consists of five 2 mm layers of lead interleaved with 5 mm layers of plastic scintillator readout at the edge by wavelength shifter bars readout by SiPMs. Each radiator layer is two radiation lengths thick. The lead sheet are covered in plastic for handling and this plastic is left intact when the lead is insterted into the stack. The whole radiator layer is encased in 1 mm thick aluminium sheet.

An engineering drawing showing the deployment of the radiator layer in one section (of four) of the MAPP-mQP detector is given in Figure 11 below. The radiator layer is divided into four parts so that each part weighs less than 100kg. Each radiator stack can be assembled form is basic components after being transported underground if need be. The purpose of the radiator layers is to tag photons and electrons.

4.3. Safety Issues Relating to Detector Installation

The MAPP-mCP) detector is designed to be installed in situ from pieces weighing a maximum of 20 kgs each, although most elements will weigh substantially less. Thus the whole MAPP-mCP detector can be taken underground

⁶<https://cds.cern.ch/record/1204301/files/CERNTHESIS-2009-062.pdf>

⁷https://jinst.sissa.it/LHC/LHCf/2008_JINST_3_S08006.pdf

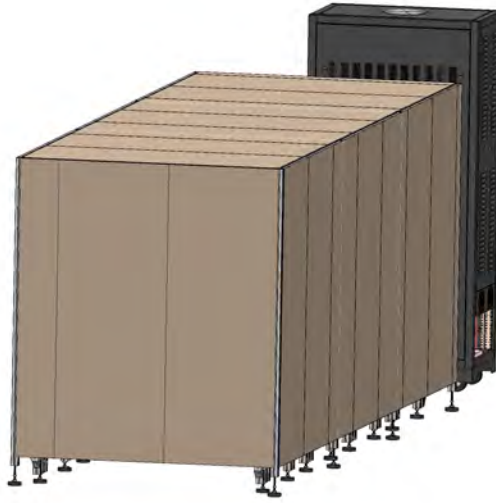


Figure 21: The aluminium flame shield completely encloses the plastic scintillator comprising the MAPP-mCP detector.

using the machine side elevator at IP8. The mass of each of the detector components is given in Appendix C. We envisage that a maximum of four people will need to be present in the UA83 gallery for installation of the MAPP Phase-1 detector. MoEDAL's installation personnel will, of course, be equipped with all the required safety gear and will operate according to the safety rules and guidelines described in the safety courses that each member of the team will have taken and passed.

4.4. Safety Monitoring After Detector Installation

The MAPP detector is readout over ethernet and does not require a team to operate it during data taking. However, it is important that the detector is monitored to ensure safe operation at all times. The safety systems that will be installed to ensure that the detector is operating safely are as follows:

- The power supplies are current limited. In addition, alarm conditions are defined that signal non-standard operating characteristics. The power supplies output and alarm conditions are monitored remotely with a feed supplied to the CERN Control Centre (CCC);
- Six temperature probes will be placed on MAPP's metal flame shield. Alarm conditions are defined that signal if any monitored temperature moves above normal ambient temperature in the UA83 tunnel. The temperature probe outputs and alarm conditions are monitored remotely with a feed supplied to the CCC.
- An IR camera will be installed on site to monitor the whole MAPP detector region. Again, the feed from the camera will be supplied to the CCC.

4.5. MoEDAL-MAPP Safety Organization

The MoEDAL-MAPP safety organization at CERN will be established prior to installation. It will consist of:

- An experimental Safety Officer (EXSO, formerly GLIMOS) as the point of contact for all experimental safety issues and communication with the EP Safety Office. The EXSO for MoEDAL for installation and the first year of running, will be the Technical Coordinator, Richard Soluk;
- Both the EXSO and the MoEDAL-MAPP Spokesperson will be available for urgent safety interventions required during the detector installation;

- All the activities of installation will be declared via IMPACT request [18] and analyzed via the usual work package analysis and VIC (Visite Inspection Commune) procedures ;
- The MoEDAL-MAPP safety files will be created on EP safety office EDMS and shared with the LHCb LEXGLIMOS. ■

5. Construction and Installation of the Phase-1 MAPP Detector

The detector will be constructed and tested at the University of Alberta. It will then be broken down to its constituent elements, none of which weigh more than 20kg, as can be seen from the complete list of parts reported in Appendix C. and then shipped to CERN for installation in the UA83 tunnel . Once situated the detector and its readout chain will be tested in situ, prior to data taking.

5.1. Organization of Construction, Installation and Running of the Detector

The two bulleted lists below describes the basic organization of the construction and installation of the Phase-1 MAPP-mCP detector:

- **Project Managers:**
 - **MoEDAL Spokesperson** - James Pinfeld;
 - **MoEDAL Technical Coordinator** - Richard Soluk;
 - **Chief engineer** - Mitchel Baker;
 - **Chief electronics engineer +Trigger and DAQ coordinator** - Paul Davis;
 - **CERN based administrator** - Veronique Wedlake;
 - **CERN based liaison with Machine** - Francois Butin
 - **EXSO(GLIMOS)** - Richard Soluk.
 - **Radiation Safety Officer** - Richard Soluk
- **Installation Crew**
 - Richard Soluk - Crew leader and responsible for mechanics installation;
 - Paul Davis - Readout electronics, power supplies and FPGA based trigger;
 - James Pinfeld - General team member to assist in all aspects of installation;
 - Phd-student/Post Doctoral student 1 - General team member to assist in all aspect of installation;
 - Phd-student/Post Doctoral student 2 - General team member to assist in all aspect of installation.

Team	Members of the team
GRAD TEAM A	M. Staelens, A Salazar-Lobs
GRAD TEAM B	M. Shaa, M. Kelly
STAFF TEAM A	M. de Montigny, P-P Ouimet
STAFF TEAM B	R. Soluk, P. Davis J. Pinfeld
Elec. Techs	P. Davis, J. Chaulk
Machinists	D. Bizuk, J. Cameron, A. Vinagreiro

Table 1: RLS team members.

5.2. Construction of the Detector

A Resource Loaded Spreadsheet (RLS) for the construction of the MAPP-mQP detector is given in Figure 22, showing the monthly view. The constitution of person-power resources mentioned in the RLS is given in Table 1. The previous schedule had to be modified for the following reasons:

- The move to new location in UA83 was not a clear possibility until June 2021;
- The UA83 location is further from IP8 and we needed to readjust the pointing geometry of the detector. This required the refabrication of the support grids and other support structures.
- We have additional Covid related delays:
 - Our PMT supplier (HZC-Photonics) ceased trading in the the spring 2021 due to Covid related financial problems and we had to order our last 100 PMTs from Hamamatsu with a 3 month lead time;
 - The delivery of our final scintillator order of 250 (half bars) from our scintillator bar supplier, Nuvia, were delayed by several months due to Covid-19 operating slowdowns.

The Hamamatsu PMT, chosen to replace the missing HZC photonics PMTs, was picked to be as close as possible in performance to the HZC tubes. The properties of the two tubes are summarized in Table 2. The Hamamatsu PMTs will be placed in the last two sections of the MAPP-mQP detector to be installed. They will be distributed in order that their response can be compared to that of the HZC-Photonics PMTs downward going cosmic and penetrating muons from IP8.

ITEM	HZC-Photonics	Hamamatsu
Model no	XP72B22	R14374
Tube Size	3-inch	3-inch
Shape	Circular	Circular
Window material	Borosilicate glass	Borosilicate glass
Photocathode	Bialkali	Bialkali
Wavelength range of max. response	300-650nm	300-650nm
Quantum efficiency	25% at 400 nm	27% at 380 nm
Gain	3×10^6	10^7
Rise time	3ns	3.5 ns
Anode dark current	10nA	50 nA
Dark counts	600 cps	-
Maximum operating voltage	1300V	1500V

Table 2: Comparison of specification of the HZC-Photonics (XP72B22) and Hamamatsu (R14374) PMTs

We can see from the resource loaded spreadsheet that the MAPP-mQP detector construction will not be finished until March 2022.

5.3. MAPP-mCP Detector Installation

Due to move of detector location, Covid-19 related delays, and HZC PMT supplier failure we propose to install the MAPP-mQP detector in two Phases:

- **Nov. 2021 Jan. 2022:** Install up to half the detector with readout electronics and take test data during 2022;
- **Winter shutdown 2022-2023:** Install the remaining portions of the detector in the contiguous Winter months of 2022/2023, for data taking with the full detector in the spring of 2023.

Funding is in place to purchase the much more expensive Hamamatsu PMTs. As the detector is now on the machine side we will not need to interface (except for parking lot issues) with LHCb, only with machine personnel. We need to finish the first part of the installation of MAPP-mCP in the UA83 tunnel by the beginning of February 2022, as UA83 will be closed for access from the end of January 2022.

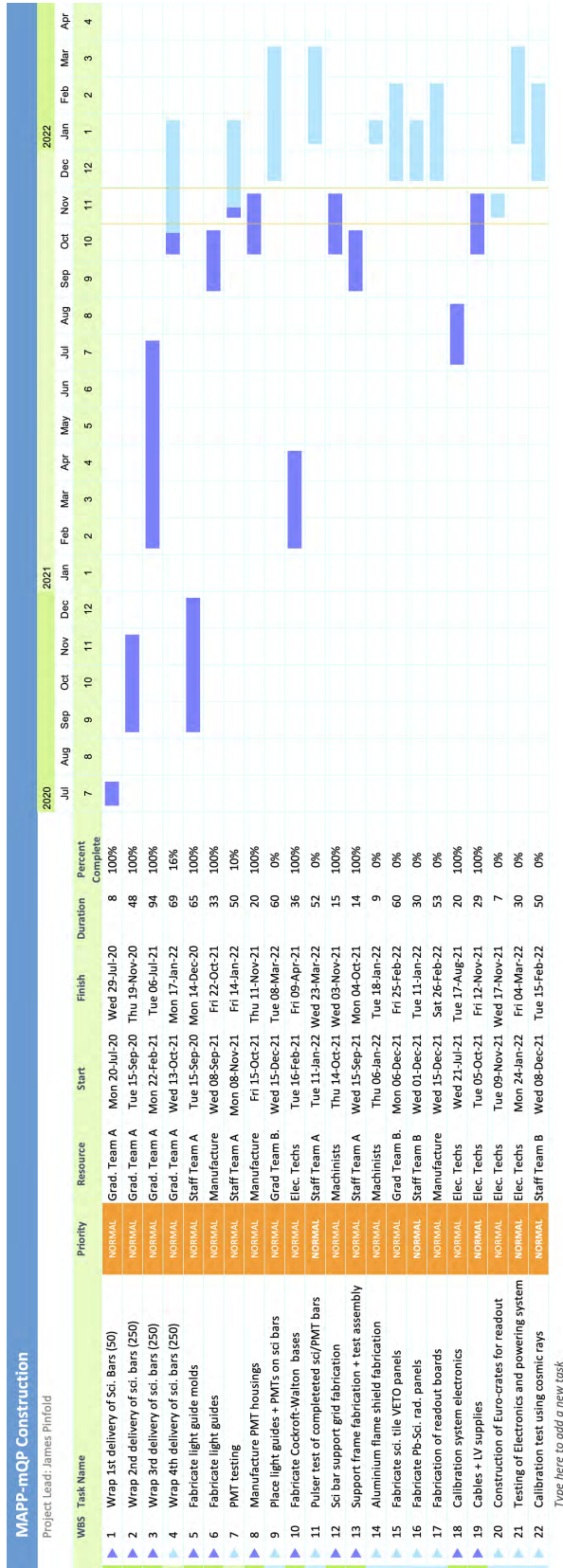


Figure 22: A Resource Loaded Spreadsheet for the construction of the MAPP-mQP detector.

6. Maintenance and Operation of the MAPP Detector During Run-3

The MAPP-mQP detector will be read out via ethernet during the run to large scale onsite disk storage at CERN. The UA83 gallery is not accessible during LHC running periods. In the event of a failure or malfunction of MAPP-mQP we will not be able to repair the detector until we have a TS, in which access to the UA83 tunnel is possible. Typically, there are a few Technical Stops (TSs) within the year besides the winter shutdowns.

We could continue running with the failure of a large fraction of the readout channels although understandably this would compromise the physics performance of the detector. In order to reduce the risk of shutdown of data taking during the run we have included in our electronics design a redundant power supply system and a redundant DAQ computer, to ensure robust operation of the overall detector.

In order to continue data taking in the event of a disruption of the ethernet connection the DAQ server will have 40TB of local disk storage. Data will be written to this disk until the ethernet connection is reestablished. During normal running the data rate will be well below 0.5 TB/day allowing an extended period of running without the need to export data to remote storage. Initially, the fewest possible restriction will be applied to the trigger and the data rate will be limited by storage write speeds.

The MAPP detector is designed to be operated remotely and to shutdown in the event that any MAPP power supply draws more than a set maximum current. Nevertheless, the MAPP detector needs to be monitored 24/7 by personnel based on site primarily for safety purposes - as described in Subsection 4.5. This is achieved by having a team of at least two MoEDAL-MAPP physicists at CERN, full-time. So that at any time there is an on-call responsible while the machine is operating and during TSs. This team would be enhanced by an average of 0.5 FTE person, formed from MoEDAL-MAPP collaboration members who are visiting CERN and have the required safety training. For planned upgrades or maintenance during running periods we will call on manpower resources described in Subsection 5.1.



Figure 23: The location of the MAPP Control Room (Bat. 17 R-007).

6.1. The MAPP Control Centre

The base of operations of the MAPP detector is the MAPP Control Centre (MCC) in Bat. 17 R-007, the location of which is shown in Figure 23. MAPP's CERN based operators have access through their on-call cell phones to the monitoring and alarm system as well as simple controls that allow them to turn off power and alert the CCC. The on-call MAPP operator and the off duty operator as well as the Technical Coordinator + Spokesperson also are connected to this system at all times via cellphone. During the day the on-call MAPP operator will usually sit in the control room. During the evening and night the on-call will be connected by cell-phone to the MAPP control and monitoring services. The on-call cellphone will be switched on at all times.

7. Funding Plans for the MoEDAL-MAPP Phase-1 Installation

The funding for the MAPP-mQP detector derives from multiple sources: an NSERC operating grant, the University of Alberta and the MoEDAL Collaboration. On May 20th we received major funding from an NSERC RTI (Research Tools and Instruments) grant (\$310K) to complete the MAPP detector. In terms of manpower, our project electronics engineer, mechanical engineer and detector technologist are funded from our existing NSERC MRS grant. We have sufficient funds in hand to deploy the MAPP-mQP detector (as described above) to take data in Run-3.

The deployment of the MAPP-mCP Outriggers will be the topic of a future addendum to this TP. However, we thought it would be useful at this stage to include funding plans for this future detector. We have received a significant donation of scintillator from EXO-200 towards the completion of the Outrigger. The funding to complete the Outrigger is being sought from the Natural Science and Engineering Council (NSERC) of Canada. If successful, the money would be available in April 2022. If the grant is not awarded we shall utilize MoEDAL-MAPP Collaboration funds to finish the work.

8. Physics Issues

In order to fully understand the sensitivity of the MoEDAL-MAPP detector to we are performing studies of a number of relevant physics benchmarks. Examples of initial benchmark studies are presented below. To complete these physics studies we need to fully and accurately simulate: the detector and its response; the passage of primary and secondary particles through the intervening infrastructure; and, the transport of cosmic ray particles through the 105 m overburden. The complete Simulation package UA83-MAPP-MoEDAL Arena (SUMMA) is discussed below.

8.1. The Full Simulation of the UA83, MoEDAL, MAPP-mCP Arena (SUMMA)

The previous version of SUMMA, with the MAPP-mCP detector deployed in the UGC1 region, was nearing completion in Spring of 2021 when the decision was made to move MAPP's location to the UA83 tunnel. The move required an extensive update to the SUMMA code to take into account the MAPP-mCP

new final position 100m away (UA83) from the IP. Additionally, the modelling of the intervening infrastructure had to be completely redone. However, the existing cosmic ray simulation module of SUMMA did not require extensive updates.

The SUMMA simulation is derived from: the final CAD drawings of the MAPP-mCP detector; accurate CAD drawings of the machine infrastructure; and, the existing model of cosmic ray transport through the overburden. In all, the simulation involves over 2500 elements. The SUMMA code will be ready for use in mid-December 2021.

The Physics Processes included in SUMMA, are:

- Primary Interaction and secondary particles, factory lists :
 - FTFP_Bert model of hadronic showers
 - QGSP_BERT_HP for neutron fluxes
- Transportation and Decay;
- Electromagnetic Interactions.
 - Gamma conversion, Compton scattering, photo-electric effect for gammas;
 - Multiple scattering, ionization, bremsstrahlung for electrons and annihilation for a positron;
 - Multiple scattering, ionization, bremsstrahlung and pair production for muons;
 - Multiple scattering and ionization for other particles.
- Scintillation processes
 - Scintillation and Cerenkov for particles;
 - Absorption, Rayleigh scattering, Mie scattering and boundary processes for optical photons.

The SUMMA ionization energy loss calculation for milli-charged particles is based on a modified Bethe-Bloch formula [22].

8.2. Some Physics Benchmarks

The physics case for the MAPP-mCP detector presented previously were all predicated on its position in the UGC1 gallery, some 55m away from IP8 with the central axis of the detector at an angle of approximately 6° to the beam-axis. In this section we will examine the effect of the move of the MAPP-mCP detector to its new location in UA83 some 100m from the IP8, at an angle of 7° to the beam-line. Despite the MAPPmCP detector's increased distance from IP8 we shall show its physics program is still competitive.

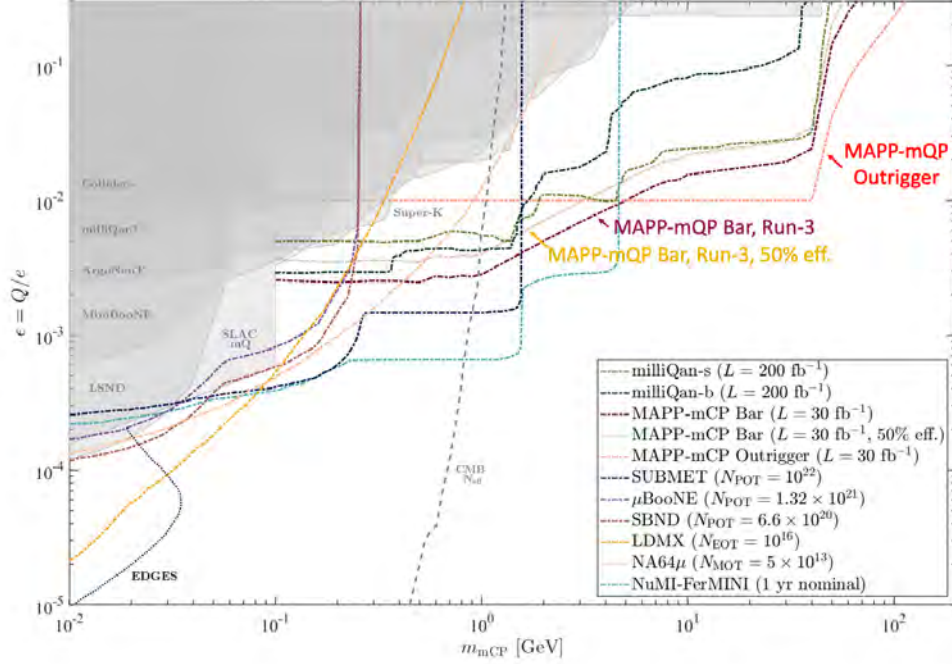


Figure 24: Direct bounds from accelerator based searches and indirect bounds from the effective number of neutrinos from Planck are shown. The projected sensitivity for mCPs, for models with a massless dark photon are presented for milliQan (for the slab (s) and bar (b) detectors and MAPP-mCP (for the MAPP-mCP bar (B) and Outrigger (O) detectors) at Run-3. The existing bounds given here are described in more detail in Ref [23].

The Outrigger detector is comprised of 4 layers of 5cm x 50cm x 60cm scintillator plates arranged in plank formation as shown in Figure 25. The purpose of the Outrigger detector is to increase MAPP-mCP's overall acceptance primarily for higher mass mCPs. An initial study of the sensitivity of the MAPP-mCP Outrigger detector is given in Figure 24.

8.2.1. Mini-Charged Particles from Dark QED

We here consider a class of Feebly Interacting Particle (FIP) that has a mini-charge (mCP) as small as $10^{-3}e$, or lower. A common scenario is from a Dark Sector model where one considers a mCP coupled through a very light kinetically mixed dark photon [20][21]. Although the mCP does not carry SM electroweak quantum numbers it behaves as a particle with a tiny electric charge. The DY process provides the main production channel for GeV-range mCPs at the LHC. The sensitivity of the MAPP-mCP detector deployed at UA83 to mini-charged particles produced in this way is shown in Figure 24.

It should be noted that in Figure 24 the detector efficiency and backgrounds have not been taken into account. We expect the limits that we can place on the DY production of mini-charged particle pairs to soften slightly when this is done, in the near future. In the meantime, in order to obtain some idea of the effect of backgrounds and detector efficiency we applied a 50% efficiency across the board to to and plotted the resulting sensitivity contour in Figure 24.

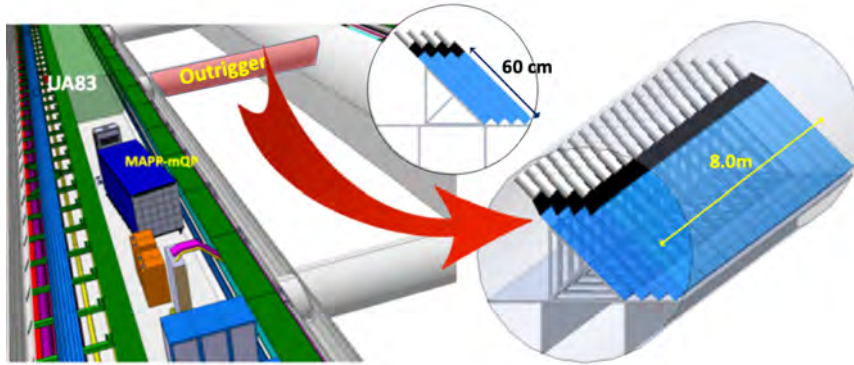


Figure 25: The proposed Outrigger detector for MAPP-mCP.

As can be seen, even with this overall “inefficiency” the MAPP-mCP is still competitive with other mCP, especially at high masses.

We are currently in the process of including a number extra channels that result in the pair production of mini-charged particles in the GeV range, from the decays of the Υ , J/ψ , $\psi(2S)$, ϕ , ρ , and ω as well as Dalitz decays of the π^0 , η , η' , and ω . When these additional channels are considered we expect our ability to probe mCP production at the LHC to be enhanced over the level indicated in Figure 24.

8.2.1.1. Backgrounds. A potential source of background mentioned previously is due to the dark count from the PMT. For the HZC-photonics the dark count rate is typically 600 cps. Considering the mCP trigger, that consists of requiring a mCP signal in 4 collinear bars in coincidence, with a trigger window of 25 ns and a beam crossing rate of 40 MHz, we would expect a trigger rate due to the dark count rate in the PMTs, of roughly 0.003, in a data-taking year of 1.5×10^7 s.

The MAPP-mCP detector is protected from cosmic ray backgrounds by a 105 m overburden. MilliQan, by comparison, is deployed near to the CMS detector at a depth of 73m. The cosmic ray background expected in the MAPP-mCP detector has been assessed by the MoEDAL-MAPP simulation group to be $(4.04 \pm 0.06) \times 10^{-5} \text{ cm}^{-2} \text{ s}^{-1}$. This amounts to about 2 muons/s incident of the top of the MAPP-mCP veto detector, with area $\sim 4.5 \text{ m}^2$. This rate is in consistent with measurements taken in the UGC1 gallery in 2018. Considering the trigger requirement for mCPs and the high efficiency of the MAPP-mCP veto system the background from uncorrelated CR muons is expected to be negligible.

The most important source of background is thought to be due to cosmic ray events with high muon multiplicity where a number of muons penetrate underground together, This has been observed, for example, by the ALICE [25] TPC with effective CR muon detection area of 17 m^2 and 28 m rock overburden, where the corresponding figures for the MAPP-mCP detector at 4.4 m^2 and 105 m. The concern is that a number of particles could impinge on the detector together increasing the probability of satisfying the mCP trigger conditions. However, the greater the multiplicity of muons impinging on the MAPP-mCP detector region, the greater the chance on of these muons would VETO the event. There are a number of additional factors that act to reduce this potential source of background;

- The rate of these showers is very small compared to the rate of single uncorrelated particles given above. For example, the ALICE data shows over six orders of magnitude fall in the number of events with a multiplicity of 20 muons compared to just a few muons.
- In order for cosmic ray muons from above or below to reach a bar and give even a small mCP signal the charged CR particle would normally need to cross two VETO counters which have an efficiency better than 99.7% and “clip” a bar. This would need to happen four times in four contiguous bars within the trigger time-window, without hits from other CR muons in the shower registering in the VETO system;
- The rate of horizontal cosmic rays is greatly suppressed compared to the downward flux. If horizontal cosmic ray muons do reach the MAPP detector they must pass through four vertical veto walls of thickness 2.5 cm that

are placed in front of MAPP and between each MAPP section, and also the back wall of the cosmic ray VETO detector of thickness 1 cm, in order to satisfy the mCP trigger;

- Neutrons associated with a muon shower can evade the VETO system and cause, for example, a nuclear recoil that can give rise to a small signal in a bar. This would need to happen in four contiguous bars within the trigger time-window. At the same time the accompanying charged particles in the shower would have to miss the VETO system.

As stated above in Section 2 we can monitor the VETO system, with collisions-off and collisions-on, for any penetration of the VETO system. If necessary we can utilize the outer layer of scintillator bars in MAPP-mCP detector as an additional VETO system.

8.2.2. Detecting the EDM of Exotic Particles

A particle with a very small electromagnetic interaction with matter via its Electric Dipole Moment (EDM) can also be considered to be a FIP. We consider here a search for a heavy neutrino member of a fourth generation lepton doublet with an EDM that may be as high as 10^{-15} e cm [26]. In this case, such a heavy neutrino would appear as an apparently fractionally charged particle in the MAPP-mCP detector, via its ionization due to the neutrino's EDM. MAPP-mCP's sensitivity to such a particle is shown in Figure 26.

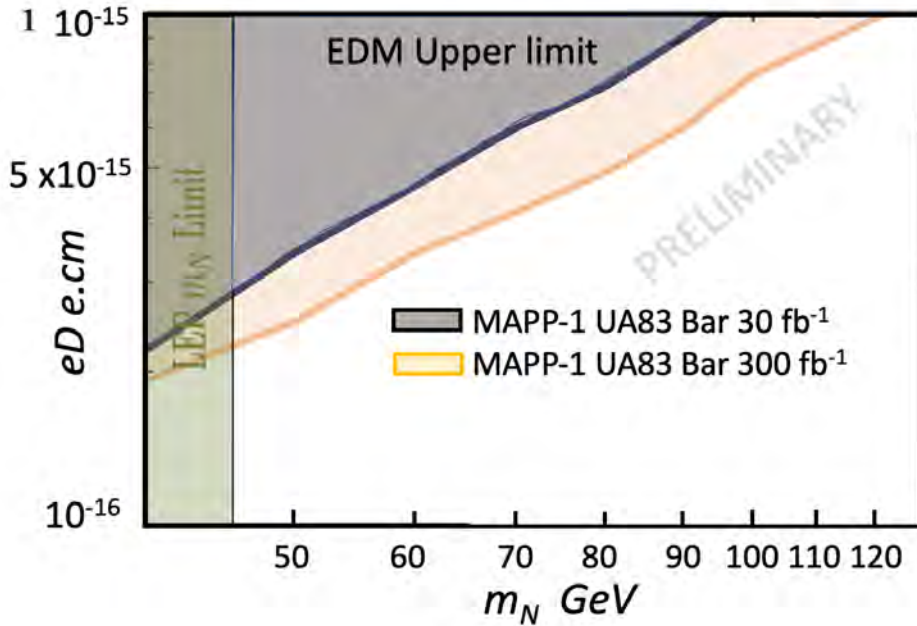


Figure 26: The reach for heavy neutrino EDM detection at MoEDALs MAPP detector at $\sqrt{s} = 14$ TeV, with 3 or more events observed at 95% C.L., and 30 fb^{-1} and 300 fb^{-1} of integrated luminosity.

In principle it is possible to distinguish between an mCP and a particle with an EDM that is large enough to be detected in a scintillator based detector. This would be done by utilizing the distinct energy deposition signatures of the two particle types. However, in practice this would be challenging as only small amounts of light are being generated in each case.

8.2.3. Searching for LLPs

Although the MAPP-mCP detector is primarily designed to search for feebly electromagnetically interacting particles (FIPs) it has some sensitivity to LLPs. For example, this sensitivity has recently been explored in Ref. [27]. In this paper it is hypothesized that dark Higgs mixing with the SM Higgs boson makes possible the direct search of the

dark Higgs inflaton at collider experiments. The Dark Higgs bosons (ϕ) can be produced at LHC in rare heavy meson decays (such as K and B mesons). They are highly collimated, boosted in the direction of the parent meson direction with decay lengths that can exceed $O(10^3)m$. Normalised detection probabilities in MAPP quoted by the author and compared to the FASER experiment, are given in Figure 27.

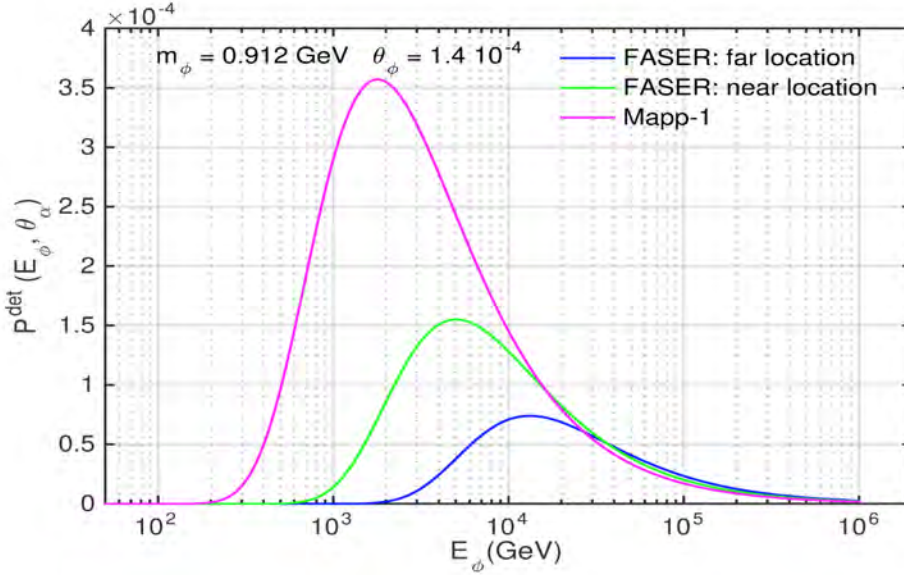


Figure 27: The dependence on the dark Higgs energy E_ϕ of the normalised detection probability corresponding to different experimental configurations obtained for cosmological best fit solution for m_ϕ and θ .

8.2.4. The Search for LLCs

In our initial LoI we described the MALL (MoEDAL Apparatus for very Long Lived Charged Particles) detector whose purpose is to search for LLCs. Our studies have shown that by placing MoEDAL's 2560 exposed trapping detector volumes, each of size 2.5 cm x 2.5 cm x 19 cm, underneath the MAPP-mCP detector we can monitor them for the decays of electrically charged particles that have stopped and been captured, obviating the need for the MALL detector. The arrangement of trapping volumes with respect to the MoEDAL-MAPP detector is shown in Figure 28. This development will be presented in detail in a future addendum to this TP in 2022. No additional issues, eg mechanical or infrastructure-related, relating to this development need to be considered here.

Operating in this mode the MALL-mCP detector can measure particle lifetimes much longer than 10 years. Both ATLAS and CMS have searched for exotic long-lived particles produced in p-p collisions. To date they have probed lifetimes up to 10 days [24]. An example of a physics arena in which extremely long-lived particles arise is that of superweakly-interacting massive particles, or superWIMPs, where the superWIMPs naturally inherit the desired relic density from late decays of metastable WIMPs [28]. Figure 29 shows that for quite reasonable values of WIMP mass and mass difference between WIMP and Super-WIMP, lifetimes well in excess of 10 years are predicted.

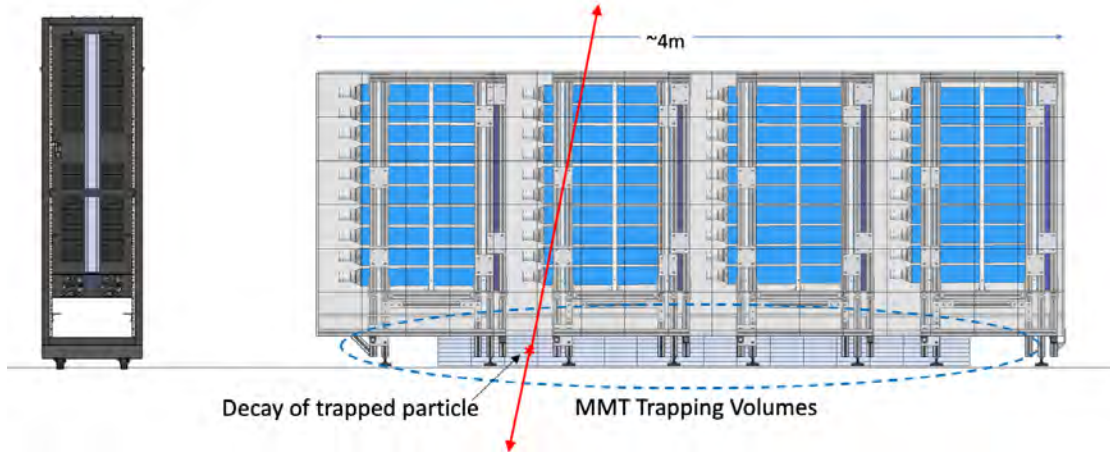


Figure 28: A depiction of the MAPP-mCP detector with the MoEDAL trapping volumes deployed.

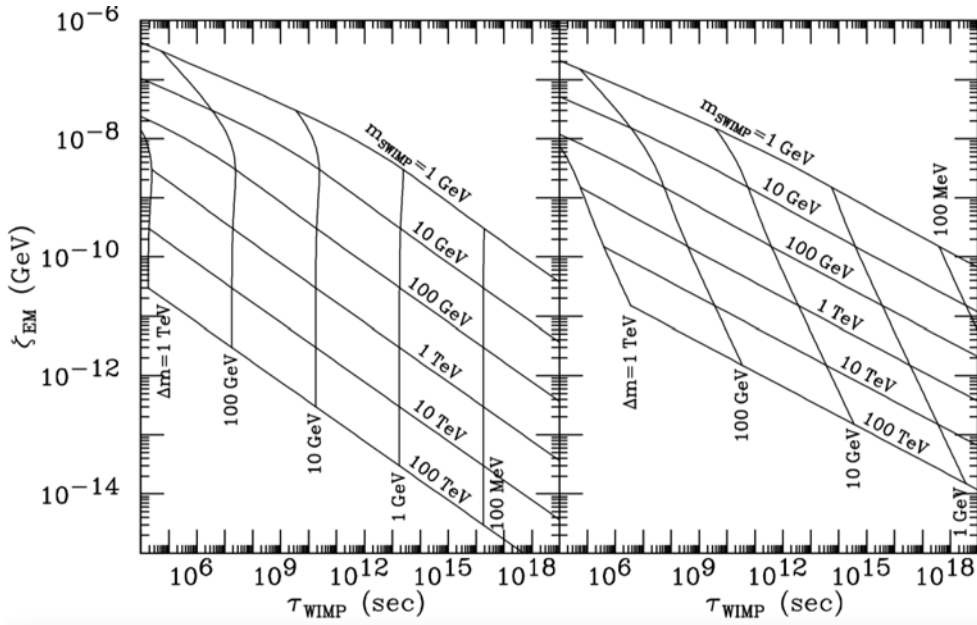


Figure 29: Predicted values of WIMP lifetime and electromagnetic energy release ζ_{EM} in the \tilde{B} (left) and $\tilde{\tau}$ (right) WIMP scenarios for $m_{SWIMP} = 1 \text{ GeV}, 10 \text{ GeV}, \dots, 100 \text{ TeV}$ (top to bottom) and $\Delta m \equiv m_{WIMP} - m_{SWIMP} = 1 \text{ TeV}, 100 \text{ GeV}, \dots, 100 \text{ MeV}$ (left to right).

9. Conclusion

In February 2020 the MAPP-mCP detector was first presented to the LHCC as a MoEDAL upgrade. Despite extensive Covid-19 related delays and a change of deployment from UGC1 to UA83 we are now poised to instal the MAPP-mCP detector for data taking in Run-3, as Phase-1 of a broader upgrade plan encompassing Run-3 and HL-LHC. The plan for installation of the Phase-1 MAPP detector (MAPP-mQP) for Run-3 data taking presented here allows a significant enhancement of the (Run-2) MoEDAL Experiment's physics reach. In particular, this upgrade extends MoEDAL's ability to detect HIP avatars of new physics to include feebly interacting (mQP) messengers of physics beyond the Standard Model with ionization power as small as a relativistic particle with electric charge $\sim 10^{-3}e$, where e is the charge of the electron. We will also utilize the MAPP-mCP detector to monitor exposed MoEDAL Trapping Detector volumes for the decays of captured LLCs, thus obviating the need for the previously proposed MALL detector. Additionally, the MAPP detector will give some limited, although useful, ability to detect neutral very long-lived particles (LLPs).

MoEDAL-MAPP will significantly enhance the discovery potential for HIP, mCP and LLP incarnations of new physics, in a manner that is complementary to the main LHC experiments, ATLAS and CMS. The MAPP-mCP detector is competitive with the milliQan detector [29] that will also be deployed for Run-3 and covers a different pseudo-rapidity range. In the event of the discovery of a mini-charged particle by MAPP-mCP and milliQan, a signal seen in two different detectors with their different systematics would provide the necessary confirmation of a discovery. Indeed, the use of multiple experiments to provide verification for important experimental findings has been adopted at LEP (ALEPH, DELPHI, L3 and OPAL) as well as the LHC (ATLAS and CMS).

Additionally, the MoEDAL and MAPP-mCP detectors working together will provide a superior sensitivity for LLCs as well as the unprecedented ability, at a collider, to detect and measure lifetimes that extend out to 10 years or more. The volume of the MAPP-mCP detector and veto system can also be used to search for LLPs. Importantly, the MAPP-mCP detector covers a different pseudo-rapidity region than FASER and in that sense provides a complementary coverage. Additionally, MAPP-mCP's limited but useful sensitivity in this arena could in some circumstances provide a confirmation of a signal observed by FASER [30].

Although the subject of a future Technical Proposal, Phase-2 of MoEDAL's plan for HL-LHC envisages data taking with MoEDAL, MAPP-mCP as well as MAPP-2. MAPP-2 would have a significantly enhanced fiducial volume taking up most of the UGC1 gallery. The necessary civil engineering and safety upgrades to UGC1 would take place in the long shutdown preceding LHC's Run-4.

The Bibliography

- [1] J. L. Pinfold et al., “Technical Design Report of the MoEDAL Experiment”, the MoEDAL Collaboration. Jun 8, 2009. 76 pp. CERN-LHCC-2009-006, MoEDAL-TDR-001.
- [2] B. Acharya et al., “Search for Magnetic Monopoles with the MoEDAL prototype trapping detector in 8 TeV proton-proton collisions at the LHC,” MoEDAL Collaboration, JHEP 1608 (2016) 067.
- [3] B. Acharya et al., “Search for Magnetic Monopoles with the MoEDAL Forward Trapping Detector in 13 TeV Proton-Proton Collisions at the LHC,” MoEDAL Collaboration, Phys. Rev. Lett. 118 (2017) no.6, 061801.
- [4] B. Acharya et al., “Search for Magnetic Monopoles with the MoEDAL forward trapping detector in 2.11 fb¹ of 13 TeV proton-proton collisions at the LHC,” MoEDAL Collaboration, Phys.Lett. B782 (2018) 510-516.
- [5] B. Acharya et al., “Magnetic Monopole Search with the Full MoEDAL Trapping Detector in 13 TeV pp Collisions Interpreted in Photon-Fusion and Drell-Yan Production,” MoEDAL Collaboration Phys. Rev. Lett. 123 (2019) no.2, 021802.
- [6] B. Acharya et al., “First search for Dyons with the full MoEDAL trapping detector in 13 TeV pp collisions,” MoEDAL Collaboration, e-Print: 2002.00861 [hep-ex], to be Published in Phys. Rev. Lett.
- [7] B. Acharya et al., “First experimental search for production of Magnetic Monopoles via the Schwinger mechanism”, under preparation.
- [8] B. Acharya et al., “First Search for Dyons with the Full MoEDAL Trapping Detector in 13 TeV pp Collisions,” MoEDAL Collaboration, Phys. Rev. Lett. 126 (2021) 7, 071801, e-Print: 2002.00861 [hep-ex].
- [9] B. Acharya et al., “First experimental search for production of magnetic monopoles via the Schwinger mechanism,” (Jun 22, 2021) e-Print: 2106.11933 [hep-ex].
- [10] B. Acharya et al., The MoEDAL Collaboration, The Physics Programme Of The MoEDAL Experiment At The LHC, Int. J. Mod Phys. A29, 1430050 (2014).
- [11] D. Felea, J. Mamuzic, R. Maselekc, N. E. Mavromatos, V. A. Mitsou, J. L. Pinfold, R. Ruiz de Austri, K. Sakurai, A. Santra, O. Vives, Prospects for discovering supersymmetric long-lived particles with MoEDAL, arXiv: 2001.05980v1 [hep-ph] 16 Jan 2020; K. Sakurai, D. Felea, J. Mamuzic, N.E. Mavromatos, V.A. Mitsou, J.L. Pinfold, R. Ruiz de Austri, A. Santra, O. Vives. Mar 26, 2019. 8 pp. IFIC/19-16, KCL-PH-TH/2019-34, Conference: C18-11-26.2 e-Print: arXiv:1903.11022 [hep-ph]. Bio. Cybern. 36, 193202. (doi:10.1007/BF00344251) (1980).
- [12] O. Pooth, S. Weingarten and L. Weinstock, Efficiency and timing resolution of scintillator tiles read out with silicon photomultipliers, JINST Vol 11 T01002 (2016).
- [13] S. Barsuk, The Shashlik electro-magnetic calorimeter for the LHCb experiment, 11th International Conference on Calorimetry in High-Energy Physics (Calor 2004).
- [14] D. Dey, J. Lee, V. Coco, C-S Moon, “Background studies for the CODEX-b experiment: measurements and simulation”, arXiv:1912.03846v1 [physics.ins-det] (2019).
- [15] J. Devine, Evelyne Dho, EP Safety Group, “Assessment for the Installation of MoEDAL MAPP-mQP Detector in UGC1 gallery for the installation of the Phase-1 MAPP detector in the UGC1 gallery, EDMS NO. 2428296, Version 1.0.
- [16] J. Devine, E. Dho, EP Safety Group, “Preliminary Ventilation Study for the Installation of MoEDAL MAPP-mQP Detector in UGC1 Gallery”, EDMS No. 2435718, Rev 1.0, Draft.
- [17] FLUKA studies for MoEDAL installation, <https://edms.cern.ch/document/2438507/1>
- [18] https://lhcb.web.cern.ch/Visiting_Pit_8/Access_request_guidelines.htm
- [19] 2631839 v.1 “Derogation to IS41 MoEDAL MAPP Experiment UA83” by Fabio CORSANEGO in status: Released Link: <https://edms.cern.ch/document/2631839/1/approvalAndComments>
- [20] B. Holdom, “Two U(1)’s and ϵ charge shifts”, Phy. Lett. B 166, p196-198 (1986).
- [21] A. Haas, C. s. Hill, E. Izaguirre, I. Yavin, “Looking for milli-charge particles with a new experiment at the LHC”, Phys. Lett. B746, p117-120 (2015).
- [22] S. Banik, V. K. S. Kashyap, M. H. Kelsey, B. Mohanty, D. H. Wright, “Simulation of energy loss of fractionally charged particles using Geant4”, NIM A971, 164114 (2020).
- [23] H. Vogel, J. Redondo, J. Cosmol. Astropart. Phys. 1402, 029 (2014).
- [24] A. A. Siryunin et al., CMS Collaboration, “Search for Decays of stopped exotic long-lived particles produced in proton-proton collisions at $\sqrt{s} = 13$ TeV,” JHEP 05, 127 (2018).
- [25] J. Adam et al., ALICE Collaboration, “Study of cosmic ray events with high muon multiplicity using the ALICE detector at the CERN Large Hadron Collider,” Journal of Cosmology and Astroparticle Physics 2016 (2016) 32.
- [26] M. Frank, M. de Montigny, P-P Ouimet, J. L. Pinfold, A. Shaa, “Searching for Heavy Neutrinos with the MoEDAL-MAPP Detector at the LHC,” Phys. Lett. B 802, 135204 (2020).
- [27] L. A. Popa, “Search for dark Higgs inflaton with curvature couplings at LHC experiments,” arXiv:2110.09392v1 [hep-ph] 18 Oct 2021
- [28] J. L. Feng, A. Rajaraman, F. Takayama, “SuperWIMP signals from the early universe,” Phys. Rev. D 68, 063504 (2003).
- [29] A. Ball et al., “Sensitivity to millicharged particles in future proton-proton collisions at the LHC with the milliQan detector,” milliQan Collaboration, Phys. Rev. D 104 3, 032002 (2021).
- [30] A. Ariga et al., FASER Collaboration, “FASER’s physics reach for long-lived particles”, Phys. Rev. D99 no.9, 095011 (2019).

1. EXISTING SITUATION AND INTRODUCTION

The MoEDAL experiment has been operating jointly with LHCb at Point 8 of the LHC since 2010, with little impact on infrastructure, mostly thanks to the joint efforts of the MoEDAL and LHCb collaborations. The MoEDAL collaboration has expressed the intention to install some new experimental setup (MAPP-mQP) in the UGC1 gallery at LHC Pt8, (see [1] and [2]). However, it appears that the amount of work needed to prepare the UGC1 gallery for installation of the MAPP-mQP detector is not compatible with data taking in 2022, nor probably in 2023. As a consequence, the LHCC recommended to look for alternative locations for the MAPP-mQP setup.

A suitable location has been identified in the UA83 gallery, both in terms of space available and operating conditions.

The installation of these new detector elements (MAPP-mQP, see Figure 1 and Figure 3) has little impact on infrastructure and no impact on either LHC or LHCb operations.

2. REASON FOR THE CHANGE

The changes are a consequence of the evolution of the MoEDAL / MAPP-mQP research programme and are intended to accommodate the evolution of the detection techniques and hardware.

The consequences of not implementing these changes would be for MoEDAL to operate the new detectors during 2022 and 2023 runs, with a great loss in data taking opportunities.

3. DETAILED DESCRIPTION

3.1 INFRASTRUCTURE REQUIRED

The space claimed for the proposed installation of the MAPP-mQP detectors is located in the UA83 tunnel, which is a former LEP klystron gallery, where free space exists, well suited for the proposed detectors (see Figure 1 to Figure 4).

The new installation will have very little impact on the infrastructure. In particular, all safety equipment is already in place:

- normal and safety lighting
- firefighting equipment (hydrant + local fire extinguishers)
- smoke detection system
- oxygen deficiency monitoring
- red phone
- general emergency stop (AUG)
- access safety system

Additional required infrastructure is limited to:

- installation of 5 new 220V 16 A power plugs, with dedicated local emergency stop (AUL), see Figure 5.

- a pair of optical fibres to be drawn from adjacent rack CYFIB01 to the MAPP detector and to the MoEDAL equipment in the UX85 cavern, see Figure 6 and Figure 7.



Figure 1 - UA83, the proposed location for the MAPP-mQP setup.

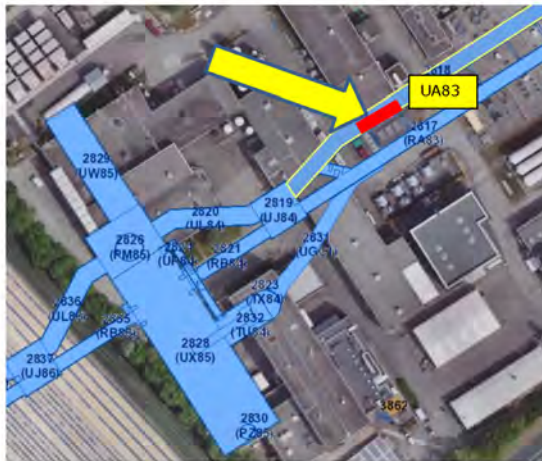


Figure 2 - The red rectangle shows the approximate location proposed for the MAPP-mQP setup in

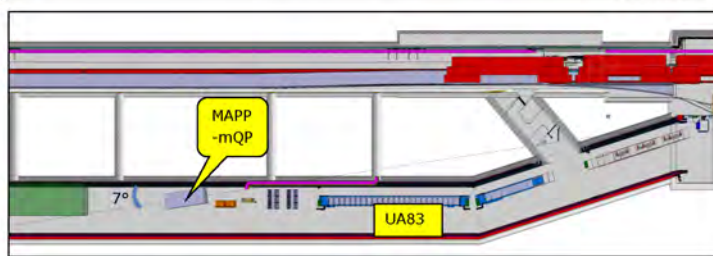


Figure 3 - Proposed layout of the MAPP-mQP setup in UA83.



Figure 4 - Indication of rough envelope of the MoEDAL-MAPP-mQP in its proposed location in UA83.



Figure 5 – Proposed location of requested 5 x 220V 16 A power plugs with dedicated local emergency stop (AUL) in UA83.

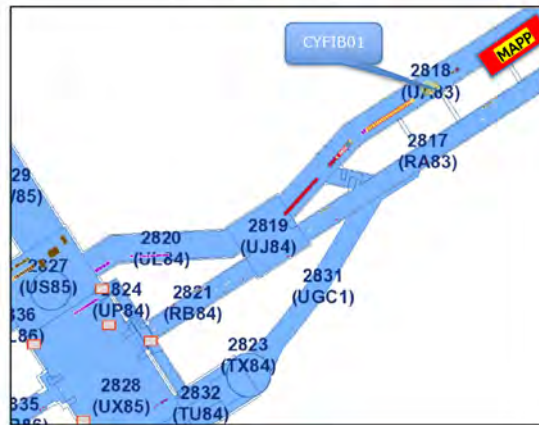


Figure 6 - Location of rack CYFIB01 in the UA83 gallery.



Figure 7 - Rack CYFIB01 in the UA83 gallery.

3.2 SPACE REQUIRED

The MAPP-mQP setup is constituted mainly of scintillators and Photo Multipliers (PMT). The overall MAPP-mQP dimensions are shown in **Error! Reference source not found.**, to be compared with the volume available in the UA83 gallery, as shown in Figure 9.

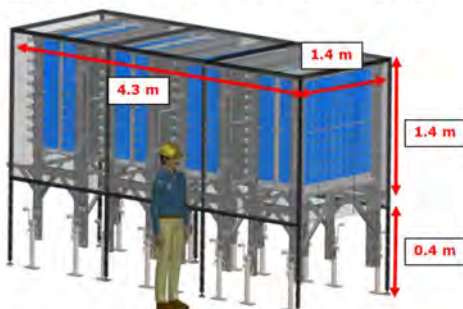


Figure 8 - Dimensions of the MAPP detector to be installed in UA83 gallery.

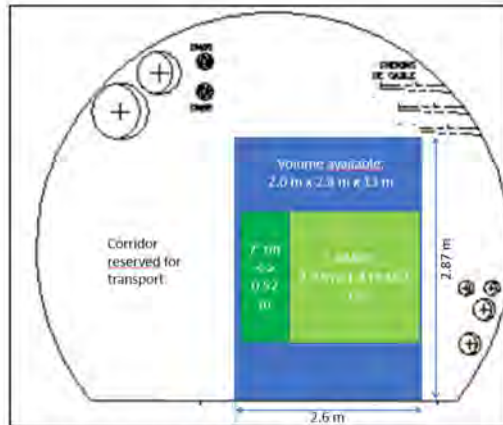


Figure 9 - Cross section of the UA83 gallery with dimensions of the free volume for the MAPP detector. 7° tilt wrt LHC axis is taken into account, see also Figure 3.

4. IMPACT ON OTHER ITEMS

4.1 IMPACT ON UTILITIES AND SERVICES

Raw water:	No Impact
Demineralized water:	No Impact
Compressed air:	No Impact
Electricity, cable pulling (power, signal, optical fibres...):	5 power plugs 220V, 16 A with dedicated AUL to be installed close to the detector: Ticket RQF1836639, by EN-EL-EWS 2 optical fibres to be pulled from rack CYF1B01 to MAPP detector in UA83 and MoEDAL detector in UX85, Ticket RQF1801156 by EN-EL-FO
DEC/DIC:	See tickets RQF1801156 and RQF1836639
Racks (name and location):	No Impact
Vacuum (bake outs, sectorisation...):	No Impact
Special transport/handling:	No Impact

Temporary storage of conventional/radioactive components:	None
Alignment and positioning:	The link to the IP8 location and tracing of beam height/directions at cm level in UA83 has been discussed and agreed with the BE-GM group.
Scaffolding:	None
Controls:	None
GSM/WIFI networks:	Available
Cryogenics:	None
Contractor(s):	None
Surface building(s):	None
Integration:	ST1471398_01, ST1479878_01
Others:	

5. IMPACT ON COST, SCHEDULE AND PERFORMANCE

5.1 IMPACT ON COST

Detailed breakdown of the change cost:	Survey: 5 kCHF Power distribution + AUL: 3 kCHF Optical fibres: 5 kCHF TOTAL: 13 kCHF
Budget code:	T299020 MoEDAL Common Fund

5.2 IMPACT ON SCHEDULE

Proposed installation schedule:	UA83 is available at any time until restart of LHC on 21 st Feb 2022, except during the pilot run (W42 and 43 in 2021). Survey + floor tracing: W44 of 2021 by BE-GM Power plugs installation: W45 of 2021 EN-EL-EWS Installation of MAPP: W 47-49 of 2021 by MoEDAL team and EN-HE
Proposed test schedule (if applicable):	Test with cosmics: Jan - Feb 2022 by MoEDAL team
Estimated duration:	2 months
Urgency:	High
Flexibility of scheduling:	Not much

5.3 IMPACT ON PERFORMANCE

Mechanical aperture:	No Impact
Impedance:	No Impact
Optics/MADX:	No Impact
Electron cloud (NEG coating, solenoid...)	No Impact
Insulation (enamelled flange, grounding...)	No Impact
Vacuum performance:	No Impact
RZE impact on performance and availability:	Background is being evaluated by A. Ciccotelli (SY-STI). Results are not available yet, but are believed to yield results adequate for MoEDAL MAPP mQD constraints.
Others:	

6. IMPACT ON OPERATIONAL SAFETY

See EDMS document 2467861 - "LSD MoEDAL - MAPP and MALL detectors"

6.1 ÉLÉMENT(S) IMPORTANT(S) DE SECURITÉ

No impact expected on any EIS

Requirement	Yes	No	Comments
EIS-Access		X	
EIS-Beam		X	
EIS-Machines		X	

6.2 OTHER OPERATIONAL SAFETY ASPECTS

What are the hazards introduced by the hardware?	<p>The experiment contains scintillators which are not 1537 compliant. A derogation is currently being prepared by HSE before the installation in UA83 (see https://edms.cern.ch/document/2631839/1). A prior derogation exists for this experiment for a similar installation in UX85 (EDMS document 893563) and the additional request has already been discussed with HSE.</p> <p>The design of the detector minimises the risk from High Voltage (HV) equipment by transferring Low Voltage (LV) power to the Cockcroft-Walton (CW) base of each Photo Multiplier Tube (PMT). The LV to HV transformation required for PMT operation is achieved in the CW PMT base. This avoids the need for HV cabling in the area of the detector.</p>
--	---

Could the change affect existing risk mitigation measures?	Not applicable
What risk mitigation measures have to be put in place?	<p>The scintillators for the detector are housed within a flame-resistant metal casing acting as a flame shield, to prevent the propagation of fire. This mitigation is considered in the context of the derogation request required from HSE. This measure is integral to the detector and does not require any external mitigation measures.</p> <p>For the handling, installation, dismantling, and other activities involving the lead plates, the measures described in Safety Guideline SG-C-0-0-3 shall be observed.</p> <p>All lead parts of MoEDAL MAPP are wrapped in a plastic scintillator sheet and encased in a Tyvek, black plastic, black tape light shield with a surrounding aluminium flame shield.</p> <p>The presence of lead (and any other chemicals) together with any eventual chemical risk assessment shall be recorded in the CERN Chemical Register for Environment, Health and Safety (CERES).</p> <p>Electrical installations shall comply with the standards which are referred in the CERN Safety Instruction IS 24 - "Regulations applicable to electrical installations". All electrical materials shall comply with the safety requirements provided in the following CERN Safety rules:</p> <ul style="list-style-type: none"> ▪ CERN Safety Instruction IS 23 - Criteria and Standard Test Methods for the Selection of Electric Cables and Wires with Respect to Fire Safety and Radiation Resistance ▪ CERN Safety Instruction IS 48 - Fire prevention for cables, cable trays and conduits. <p>The supporting structure for the experiment must be designed in accordance with Eurocodes. In particular, load conditions and combinations shall be defined in accordance with the NF-EN-1990 and NF-EN-1991 (all applicable parts). Safety verifications of the steel elements and joint-connections shall comply with the NF-EN-1993 (all applicable parts). Any anchorage to the floor slab should also be checked and calculated with NF-EN-1992-4. A structural calculation note must be provided. Execution of steelworks shall be conformed to the NF-EN-1090 (parts 1 and 2).</p> <p>Conventional waste, such as plastic for packaging, metals for preliminary works in the framework of this project, etc. shall be handled from its collection to its recovery or disposal according to the procedures set up by SCE Department (cf. SCE website or the guide on waste management at CERN EDMS 2341248). The measures to implement shall be:</p> <ul style="list-style-type: none"> ▪ Define an adequate area for waste storage. ▪ Provide skips adapted to the type and quantity of waste expected (metals, cardboard, etc...) with clear and visible recycling panels. ▪ Regularly inspect the worksite to ensure the sorting. ▪ Inform workers about waste management procedures put in place.
Safety documentation to update after the modification	EP and MoEDAL collaboration will provide the experiment safety related documentation and will take care of the experiment safety file.
Define the need for training or information after the change	Self-rescue mask training will be required for members of the experiment collaboration wishing to access the detector in UA83.

7. WORKSITE SAFETY

See EDMS document: [1155899](#) - "Working on the CERN Site".

7.1 ORGANISATION

Requirement	Yes	No	Comments
IMPACT – VIC:	Yes		Will be organized 2 weeks before installation is due to start, after reception of an installation method statement.
Operational radiation protection (surveys, DIMR...):		X	
Radioactive storage of material:		X	
Radioactive waste:		X	
Non-radioactive waste:		X	
Fire risk/permit (IS41) (welding, grinding...):		X	
Alarms deactivation/activation (IS37):		X	
Electrical lockout:		X	
Others:		X	

7.2 REGULATORY INSPECTIONS AND TESTS

Requirement	Yes	No	Responsible Group	Comments
HSE inspection of pressurised equipment:		X		
Pressure/leak tests:		X		
HSE inspection of electrical equipment:	Yes		EN & EP	Infrastructure elements (EN) to be inspected by HSE, Detector installation (EP) also requires inspection by HSE before operation.
Electrical tests:	Yes		EP-SO/MoEDAL	AUL Test to be performed before operation of the detector
Others:		X		

7.3 PARTICULAR RISKS

Requirement	Yes	No	Comments
Hazardous substances (chemicals, gas, asbestos...):		X	

Work at height:		X	
Confined space working:		X	
Noise:		X	
Cryogenic risks:		X	
Industrial X-ray (<i>hrs radio</i>):		X	
Ionizing radiation risks (radioactive components):		X	
Others:		X	

8. FOLLOW-UP OF ACTIONS BY THE TECHNICAL COORDINATION

Action	Done	Date	Comments
Carry out site activities:			
Carry out tests:			
Update layout drawings:			
Update equipment drawings:			
Update layout database:			
Update naming database:			
Update optics (MADX)			
Update procedures for maintenance and operations			
Update Safety File according to EDMS document 1177755:			
Others:			

9. REFERENCES

- [1] J.L. Pinfeld, MoEDAL-MAPP Collaboration, "Results and future plans of the MoEDAL(-MAPP) experiment", Ninth workshop of the LLP Community, May 25-27, 2021, <https://indico.cern.ch/event/980853/contributions/4360784/attachments/2250540/3817571/LLP-Workshop%202021.pdf>
- [2] B. Acharya et al., MoEDAL-MAPP Collaboration, "MoEDAL-MAPP a Dedicated Search Facility at the LHC",



REFERENCE
LHC-XBMAPP-EC-0001

EDMS NO.	REV.	VALIDITY
2617044	0.2	DRAFT

Page 13 of 13

https://www.snowmass21.org/docs/files/summaries/EF/SNOWMASS21-EF9_EF8_James_Pinfold-088.pdf

B. Safety Derogation Request

EDMS 2631839 v.1 status Released access Restricted
PDF from EDMS_2631839_MoEDAL_IS41_derogallon_material_ffire_v1.docx modified 2021-10-06 09:27

HSE
 Occupational Health & Safety
 and Environmental Protection Unit

Safety Derogation Request Form		
Date	Requested by	Dpt/Group
27 août 2021	MoEDAL- MAPP Experiment EP Safety Office	EP

DESCRIPTION OF THE REQUEST																																																																						
Location / Project : UA83																																																																						
Regulation related to the derogation: Plastic materials needed for the MoEDAL Detector are not conforming to CERN IS41, and specifically needed due to their physical properties.																																																																						
Brief description of the Detector : The MAPP detector is comprised of 400 x (10 cm x 10 cm x 75 cm) scintillator bars, wrapped in Tyvek and then black tape. Each bar is connected via a short light guide to a 3-inch PMT. The bars are arranged in 4 sections, each with 100 bars with overall sensitive area of 1m ² . The scintillator bars (NUVIA polystyrene based scintillator) in each section are held in a square array by three support grids made of High-Density Polyethylene (HDPE). A drawing of one of the basic HDPE support grids is shown in Figure 1. The grid separates the bars one from the other by 5m to 7 mm. The air fills the interstices between the scintillator bars.																																																																						
<thead> <tr> <th>PLATE NUMBER</th> <th>DRY D-2000</th> <th>DRY C</th> <th>DRY B</th> <th>DRY A</th> </tr> </thead> <tbody> <tr><td>20</td><td>112.47</td><td>1.00</td><td>1</td><td>1</td></tr> <tr><td>21</td><td>113.01</td><td>1.01</td><td>1</td><td>1</td></tr> <tr><td>22</td><td>113.53</td><td>1.02</td><td>1</td><td>1</td></tr> <tr><td>23</td><td>113.95</td><td>1.03</td><td>1</td><td>1</td></tr> <tr><td>24</td><td>114.45</td><td>1.04</td><td>1</td><td>1</td></tr> <tr><td>25</td><td>114.15</td><td>1.05</td><td>1</td><td>1</td></tr> <tr><td>26</td><td>114.45</td><td>1.06</td><td>1</td><td>1</td></tr> <tr><td>27</td><td>115.04</td><td>1.07</td><td>1</td><td>1</td></tr> <tr><td>28</td><td>115.57</td><td>1.08</td><td>1</td><td>1</td></tr> <tr><td>29</td><td>115.77</td><td>1.09</td><td>1</td><td>1</td></tr> <tr><td>30</td><td>116.22</td><td>1.10</td><td>1</td><td>1</td></tr> <tr><td>31</td><td>116.74</td><td>1.11</td><td>1</td><td>1</td></tr> <tr><td>32</td><td>116.91</td><td>1.12</td><td>1</td><td>1</td></tr> </tbody>	PLATE NUMBER	DRY D-2000	DRY C	DRY B	DRY A	20	112.47	1.00	1	1	21	113.01	1.01	1	1	22	113.53	1.02	1	1	23	113.95	1.03	1	1	24	114.45	1.04	1	1	25	114.15	1.05	1	1	26	114.45	1.06	1	1	27	115.04	1.07	1	1	28	115.57	1.08	1	1	29	115.77	1.09	1	1	30	116.22	1.10	1	1	31	116.74	1.11	1	1	32	116.91	1.12	1	1
PLATE NUMBER	DRY D-2000	DRY C	DRY B	DRY A																																																																		
20	112.47	1.00	1	1																																																																		
21	113.01	1.01	1	1																																																																		
22	113.53	1.02	1	1																																																																		
23	113.95	1.03	1	1																																																																		
24	114.45	1.04	1	1																																																																		
25	114.15	1.05	1	1																																																																		
26	114.45	1.06	1	1																																																																		
27	115.04	1.07	1	1																																																																		
28	115.57	1.08	1	1																																																																		
29	115.77	1.09	1	1																																																																		
30	116.22	1.10	1	1																																																																		
31	116.74	1.11	1	1																																																																		
32	116.91	1.12	1	1																																																																		

| *Figure 1: The drawing of one of 12 HDPE support grids of the MAPP-MCP detector* |

The weight of the scintillator in each section is supported by an aluminium T-bar support structure and a 0.5 cm aluminium plate that forms the base of each section. Additionally, each section is protected from the other by the lead-scintillator radiator plane that includes 2 x 1 mm of aluminium sheet and 5 x 2mm layers of lead. The active detector is completely encapsulated in VETO detectors comprised of 1 cm thick acrylic scintillator (EJen-200 PVT based scintillator), with area roughly 30m². The above arrangement is shown in Figure 2. The support structures and metal plate elements are shown in blue. The HDPS support grids and metal support structures are further emphasized in Figure 3.

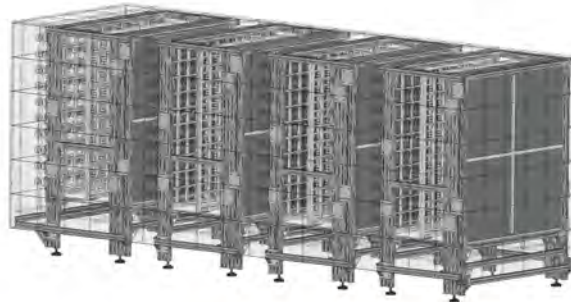


Figure 2: The basic structures of the MAPP-mQP with the outer VETO layer and the support structures emphasized.



Figure 3 The basic structures of the MAPP-mQP without the outer VETO layer the support structures emphasized.

The MAPP detector and VETO layer are completely enclosed in the MAPP-mQP flame shield as shown in Figure 3. The size of the shield is roughly 1.3 x 1.5 x 4m. The flame-shield is fabricated out

of 1mm thick aluminium sheet and has a total area of $\sim 30 \text{ m}^2$. The aluminium encloses the plastic scintillator completely. There is no break in the flame shield for cable exit. The cables exit via a patch panel.



Figure 4 The flame shield around the MAPP-mQP detector

In order to provide a hermetic environment all joints in the flame shield are sealed using heavy duty aluminium tape shown in Figure 5. Any fires within the flame shield volume would be suppressed due to lack of oxygen. The slight electrical heating arising from the PMT bases within the volume of the flame shield – the only electrical elements in the region - amounts to a few hundred Watts that is dissipated by conduction and radiation from the flame shield surface

The foreseen location in UA83 is shown in Figure 5 and Figure 6 here below.



Figure 5: Proposed location in UL83



Figure 6: Proposed layout of the MAPP-mQP setup in UA83.

Further details on the materials used and other cases of applications at CERN are available in the document: **"Information Relating to Safety of the MAPP Detector With Respect to Flammability"** From J. Pinfold, available in this same EDMS node.

Further details on the installation in the UA83 are given in the ECR "LHC-X8MAPP-EC-0001 MoEDAL MAPP mQP detector in UA83" (EDMS 2617044).



Figure 7 Heavy duty aluminium tape (0.25 mm thick), used to seal the flame shield

Gap compared with the reference regulation

Description:

Materials specifically needed for the MoEDAL Detector in virtue of their physical properties are not conforming to CERN IS 41:

Polystyrene (PS)

https://edms.cern.ch/ui/file/2631839/1/Polystyrene_Material_Data_Sheet-AMCRYS.pdf



<p>High Density Polyethylene (HDPE) https://edms.cern.ch/ui/file/2631839/1/Recycled_HDPE_Material_Safety_Data_Sheet.pdf</p>	
<p>Polyvinyl Toluene (PVT) https://edms.cern.ch/ui/file/2631839/1/EJ-200-SDS_PVT_Material_Safety_Data_Sheet.pdf</p>	
<p><u>Cause and justification of the gap:</u> PS is required for the operation of scintillation detectors in order to perform physics in MoEDAL Experiment</p>	
<p>Quantity : (kg or m³) 3,000 kgs of PS HDPE 326kg PVT 406kg</p>	<p>Dimensions : (length, width, diameter, thickness) PS: 10 x 10 x 75 cm / 100 units x 4 HDPE: support spacers grids –various measures described in Figure 1 PVT: set of plates, 1cm thick, total 30m²</p>
<p>Ignition sources: Low Voltage circuitry Distance to the nearest external powered system: An uninterruptible power supply, part of other LHC equipment, is at a distance ~1.5 m</p>	
<p>Are there other previous derogation requests for the equipment/building/installation...? Not for this installation (A previous derogation has been made for MoEDAL in UX85 EDMS 893563)</p>	
<p>What are the alternatives that have been investigated and why were they not put into place ? The scintillators for the detector are housed within a flame-resistant metal casing, to prevent the propagation of fire. This mitigation is considered in the context of the derogation request required from HSE. This measure is integral to the detector and does not require any external mitigation measures. The material properties of PS are required for scintillator detectors of this type, no other alternative is possible.</p>	
<p>Documents provided by the requestor: click or tap here to enter text.</p>	

APPLICABLE SAFETY DOMAIN		
<i>(a single domain per derogation)</i>		
<input type="checkbox"/> Mechanical (pressure, lifting, machines, HVAC, ...) <input type="checkbox"/> Cryogenics <input type="checkbox"/> Structural, civil engineering <input checked="" type="checkbox"/> Fire Safety <input type="checkbox"/> Chemical	<input type="checkbox"/> Workplace <input type="checkbox"/> Flammable gas <input type="checkbox"/> ODH <input type="checkbox"/> Electrical <input type="checkbox"/> Noise	<input type="checkbox"/> Non-ionising radiation <input type="checkbox"/> Environmental protection <input type="checkbox"/> Others: <input type="checkbox"/> click or tap here to enter text.



SPECIALIST OPINION

Specialist:

Fabio CORSANEGO HSE-OHS-IB Jonathan Guiley HSE-OHS-PE

Specialist opinion:

Acceptable with the conditions agreed here below

Compensatory measures defined in collaboration with the requestor:**safeguards: hardware/software interlocks**

power supplies are low voltage (24V), are current and temperature limited (turn off when current or temperature goes out of range) and provide an alarm signal when current or voltage moves out of some predefined operating window.

handover of alarms generated by the system

Three types of warning/alarm information will be provided to the CCC:

- 1) The current/voltage and temperature readings/alarms from the power supplies,
- 2) The hermetic metal flame shield is monitored by temperature sensors placed on the outside of the shield. The output of these temperature sensors will also be provided to the CCC,
- 3) There is a plan (not yet confirmed) to monitor the detectors + electronics with an IR camera whose output is provided to the CCC.

Other safeguards:

- 1) The power supplies, readout electronics and other non MoEDAL live equipment present in UA83 are separated by a distance of 1.5 m from the detector;
- 2) The only entities that use power in the detector volume are PMT bases. Power supplied to the bases is LV and only stopped up in the base.
- 3) The detector volume is completely encased in a hermetic (sealed to exclude air movement) flame shield. Cables enter the volume via a patch panel. Metal planes separate each of the four compartments of the detector. A strong metal plate forms the base of the scintillator bar compartments.

Conditions for the validity of the derogation :

- Temporary derogation - expiry date : [Click on document number](#)
- Permanent derogation

Description of the conditions for retaining validity:

Observance of the conditions defined in this document

Documents applicable to the reply:

TRACEABILITY

Reference and version EDMS : <https://edms.cern.ch/document/2631839/1>

STATUS OF THE DEROGATION

See EDMS

C. List of parts for the Phase-1 MAPP detector (MAPP-mQP)

Parts list for MAPP Inner Detector (Fasteners not Included)
REVISION B

Part Number	Length (mm)	Weight (kg)	Quantity	Description
80/20 STOCK PARTS FOR INNER FRAMES				
40-4040	1300	3.09	40	T-slotted profile
40-4040	1365	3.24	40	"
40-4040	1150	2.73	40	"
40-4040	778	1.85	32	"
40-4040	489	1.16	16	"
40-4040	1285	3.05	8	"
40-4040	100	0.24	16	T-slotted profile with M8x1.25 end tap
40-4336	N/A	0.13	56	45 deg corner bracket
40-4481	N/A	0.12	128	L joining plate, 5-hole
33470	N/A	0.03	120	Hidden 90 deg corner connector
40-2555	640	1.42	16	45 deg support
40-2425	N/A	0.05	16	Panel mounting block
40-2535	320	0.66	16	45 deg support
40-4307	N/A	0.05	16	Joining plate, 2-hole
TBD	N/A		1296	T-nuts and screw pairs
40-8080	2100	13.36	4	T-slotted profile for detector base
SHIELD				
40-4040	1500	3.57	12	T-slotted profile
40-4040	2800	6.66	10	"
40-4040	1800	4.28	7	"
40-4040	840	2.00	4	"
TBD	N/A	9.06	24	Mu metal panel, side
TBD	N/A	9.74	9	Mu metal panel, top
TBD	N/A	5.33	10	Mu metal panel, bottom
TBD	N/A	2.28	8	Mu metal panel, bottom sides
TBD	N/A	3.60	1	Mu metal panel, bottom front end
TBD	N/A	3.54	1	Mu metal panel, bottom back end

Part Number	Weight (kg)	Quantity	Description
CUSTOM FRAME PARTS (80/20 MAY BE ABLE TO MAKE THESE)			
04-005-M012	0.16	48	H joining plate, 4-hole
04-005-M013	16.95	8	Base plate
04-005-M014	0.37	4	Center guide
04-005-M016	0.54	8	Veto base plate
04-005-M015	0.16	32	Square joining plate, 4-hole
VENDOR OPTIONAL			
TBD		8	Screw, M8x1.25 x 20-30mm long
TBD		12	Screw, M6x1 x 15mm long
PRIMARY SCINTILLATORS			
TBD	7.73	400	Scintillator Block
TBD	0.71	400	PMT
TBD	0.24	400	Silicone Light Guide
TBD	0.08	400	PMT Cover

Parts list for 1 (out of 4) frames for the MAPP inner detector
REVISION B

80/20 STOCK PARTS				
Part Number	Length (mm)	Quantity	Description	
40-4040	1300	10	T-slotted profile	
40-4040	1365	10	"	
40-4040	1150	10	"	
40-4040	778	8	"	
40-4040	489	4	"	
40-4040	1285	2	"	
40-4040	100	4	T-slotted profile with M8x1.25 end tap	
40-4336	N/A	14	45 deg corner bracket	
40-4481	N/A	32	L joining plate, 5-hole	
33470	N/A	30	Hidden 90 deg corner connector	
40-2555	640	4	45 deg support	
40-2425	N/A	4	Panel mounting block	
40-2535	320	4	45 deg support	
40-4307	N/A	4	Joining plate, 2-hole	
TBD	N/A	324	T-nuts and screw pairs	
CUSTOM PARTS (80/20 MAY BE ABLE TO MAKE THESE)				
Part Number	Quantity	Description		
04-005-M012	12	H joining plate, 4-hole		
04-005-M013	1	Base plate		
04-005-M014	1	Center guide		
04-005-M016	2	Veto base plate		
04-005-M015	8	Square joining plate, 4-hole		
VENDOR OPTIONAL				
TBD	8	Screw, M8x1.25 x 20-30mm long		
TBD	12	Screw, M6x1 x 15mm long		